# Loss of altruism in the social amoeba *Dictyostelium discoideum* is associated with the G protein-coupled receptor, *grlG*

Laura M. Walker[*], Rintsen N. Sherpa[†], Sindhuri Ivaturi[*], Debra A. Brock[*], Jason R. Walker[‡], Joan E. Strassmann[*] and David C. Queller[*]

[*]Department of Biology, Washington University, St. Louis, Missouri 63130

[†]Department of Computational Medicine and Bioinformatics, University of Michigan, Ann Arbor, MI 48109

[‡]McDonnell Genome Institute, Washington University School of Medicine, St. Louis, Missouri 63130

**ORCID IDs:** 0000-0003-0837-7227 (L.M.W.); 0000-0002-4349-5854 (D.A.B.); 0000-0001-7547-5789 (J.R.W.); 0000-0003-0638-8440 (J.E.S.); 0000-0002-5464-1984 (D.C.Q)

**Abstract**

Aggregative multicellularity relies on cooperation among individual cells to form a multicellular body. In *Dictyostelium discoideum* this cooperation is maintained by high relatedness. Previous work showed that experimental evolution under low-relatedness resulted in an increase of cheaters (cells that contribute proportionally more to viable spores than to the dead, sterile stalk) and that many clones completely lost cooperation and the ability to form fruiting bodies.

Here, we investigate the genetic basis underlying the evolution of the cheating phenotype using whole-genome sequencing and variant analysis of these 24 previously evolved *D. discoideum* lines. We identified 38 single nucleotide polymorphisms in 29 genes, none of which have been previously reported to cause cheating and most of which are uncharacterized. Each gene has one unique variant except for the G protein-coupled receptor *grlG*, which has at least one variant in over half of the lines. Upon identifying the parallel evolution of *grlG*, we screened additional clones to investigate the correlation between variants in the gene and the complete loss of cooperation (identified by the inability to form a fruiting body). We found that variants in the first half of *grlG* that impact the signal peptide or extracellular binding domain are significantly associated with the complete loss of cooperation (non-fruiting); the association was not significant in the second half of the gene. Our results suggest that the loss of *grlG* was adaptive under the experimental conditions of low-relatedness and that the first half of the gene in particular is involved in cooperation and multicellular development in *D. discoideum*. This represents a new selfish mutation that arose naturally under conditions of low-relatedness and helps confirm the importance of high relatedness in the evolution of altruism in the social amoeba *Dictyostelium discoideum.*

**Key words:** Aggregative multicellularity, *far2*, Glutamate receptor-like protein, Orphan GPCR,

## Introduction

45 High relatedness is crucial for the maintenance of cooperation in multicellularity. Without high
46 relatedness to reduce conflict among individuals in a cooperative group, cheaters can evolve
47 that exploit the individual and destabilize altruistic traits (Hardin 1968; Gilbert *et al.* 2007). High
48 relatedness is easily achieved within organisms that go through a single-cell bottleneck or are
49 otherwise clonal, as is true for most of the more than 20 transitions from unicellularity to
50 multicellularity (Grosberg and Strathmann 2007; Knoll 2011). A single-cell origin ensures that all
51 cells are highly related (genetically identical) which reduces conflict, protects against cheaters
52 and promotes the division of labor that is so crucial for complex multicellularity such as in
53 plants and animals (Grosberg and Strathmann 2007; Cooper and West 2018). However, a single-
54 cell origin is not the only way to achieve multicellularity and its many benefits. Many other
55 organisms from across the tree of life achieve multicellularity via aggregation or fusion of
56 individual cells (Bonner 1998; Sebé-Pedrós *et al.* 2017). In this form of multicellularity, called
57 aggregative multicellularity, the cells that aggregate need not be related, so other mechanisms
58 are required to reduce conflict and maintain cooperation (Queller 2000).
59
60 Organisms that arise by aggregation offer important opportunities for evolutionary and
61 mechanistic studies of conflict and cooperation. Genetic indications of conflict and its control
62 are likely to be evident in multicellular organisms that arise by aggregation. Unlike multicellular
63 organisms that require a single-cell bottleneck, in organisms with aggregative multicellularity it
64 is possible to experimentally manipulate intra-organismal relatedness and study the outcome.
65 Among the best studied organisms with aggregative multicellularity is the social amoeba
66 *Dictyostelium discoideum.* Usually free-living in the soil, when faced with starvation *D.*

67 *discoideum* amoebae aggregate to cooperatively form a multicellular fruiting body in which
68 about 80% develop into reproductive spores and the remaining 20% die forming a stalk (Kessin
69 2001). The stalk lifts the spores, facilitating dispersal (smith *et al.* 2014). Stalk formation is
70 altruistic because cells that contribute to the stalk die, sacrificing themselves to aid in spore
71 dispersal. This partitioning of reproductive spores and sterile stalk cells provides an opportunity
72 for clones to cheat in mixtures of genotypes by contributing more than their fair share of cells
73 to spores versus the stalk (skewing the typical distribution) (Strassmann *et al.* 2000).
74
75 *Dictyostelium discoideum* is a particularly valuable and tractable model system for studying
76 aggregative multicellularity (Strassmann and Queller 2011; Ostrowski 2019). In the laboratory
77 we can experimentally manipulate populations of genetically distinct amoebae and they will
78 aggregate together and develop into a fruiting body. An extensive set of experimental tools and
79 resources (fluorescent labels, reference genome, etc.) are available that allow us to track the
80 outcome of the distinct genotypes (Buttery *et al.* 2013). In the multicellular fruiting bodies that
81 result from mixing experiments, it is usually possible to identify a winner (the clone contributing
82 more to spores than stalk) and a loser (the clone contributing more to the stalk than spores)
83 (Strassmann *et al.* 2000; Fortunato *et al.* 2003a; Buttery *et al.* 2009; Wolf *et al.* 2015; Madgwick
84 *et al.* 2018). Evidence suggests that cheating occurs in natural populations too. Despite the high
85 relatedness in natural populations (Gilbert *et al.* 2007), distinct clones are often found in close
86 proximity and they too will aggregate and form chimeric fruiting bodies (Strassmann *et al.*
87 2000; Fortunato *et al.* 2003b; smith *et al.* 2016).
88

89 Genetic mutations that result in a selfish trait such as the preferential formation of spores
90 versus stalk (cheater mutations), may pose a threat to cooperation depending on the context in
91 which they arise. Within an individual fruiting body a cheater mutation can be favored by
92 selection and contribute disproportionately more to spores than to stalk (Strassmann *et al.*
93 2000). But the outcome more broadly will depend on the relatedness of aggregating cells and
94 the extent to which those carrying the mutation can still cooperate on their own. If a clone
95 carrying the cheater mutation has completely lost cooperation such that it can only form spores
96 (an obligate cheater), then it can only persist when an exploitable clone is available. When an
97 obligate cheater clone finds itself alone without others to form a stalk, multicellular fruiting
98 body formation (development) comes to a halt resulting in a mound of cells that cannot
99 disperse, and thus a fitness of zero. We call these obligate cheater clones "non-fruiters." If
100 instead, a clone carrying the cheater mutation can still cooperate and can modify its strategy
101 depending on the availability of exploitable clones then the mutation may persist without
102 threatening the collapse of multicellularity. We call these clones “facultative cheaters.”
103
104 It has been experimentally shown that selection under low relatedness increases the
105 occurrence of both facultative (Santorelli *et al.* 2008) and non-fruiting obligate cheaters (Ennis
106 *et al.* 2000; Kuzdzal-Fick *et al.* 2011). When obligate cheaters arise in the wild where
107 relatedness is high, they should not persist because they will usually find themselves in clonal
108 or nearly clonal aggregations where their cheating advantage will not trump the disavantage of
109 their inability to form fruiting bodies on their own (Fortunato *et al.* 2003b; Gilbert *et al.* 2007).
110 In line with that expectation, no obligate cheaters have been identified from natural

populations of *D. discoideum*. While it is true that non-fruiting clones would be missed with traditional isolation techniques (Cavender and Raper 1965), Gilbert *et al.* (2007) screened specifically for the presence of non-fruiting obligate cheaters by clonally plating over 3,000 spores from wild-collected fruiting bodies to observe the phenotype. No clones were found that were incapable of forming a fruiting body. These findings are in line with predictions of kin selection theory (Hamilton 1964) and show that high relatedness helps stabilize altruism in *D. discoideum.* The altruistic trait of stalk formation can be maintained only if the benefits are shared with related individuals who likely share the altruism allele.

One way in which organisms with aggregative origins of multicellularity maintain high relatedness and the resulting cooperation is through kin discrimination (West *et al.* 2006). Kin discrimination describes mechanisms that allow individuals to identify and preferentially direct benefits to relatives and either harm or ignore non-relatives (Tsutsui 2004; Strassmann *et al.* 2011). Some species of Dictyostelids have robust kin discrimination systems that aid in the sorting of different genotypes into mostly clonal fruiting bodies (Mehdiabadi *et al.* 2006, 2009; Sathe *et al.* 2014). *Dictyostelium discoideum* also has kin discrimination with sorting regulated by two highly variable cell adhesion genes, *tgrB1* and *tgrC1* (Benabentos *et al.* 2009; Hirose *et al.* 2011; Gruenheit *et al.* 2017). Segregation by kin discrimination in *D. discoideum* takes place during early aggregation but is not maintained and does not result in fruiting bodies that are highly sorted by relatedness (Flowers *et al.* 2010; Gilbert *et al.* 2012). So although it may limit some cheaters from invading (Ho *et al.* 2013), kin discrimination alone is not strong enough to provide complete protection from selfish cheaters in *D. discoideum*. Instead, high relatedness in

133 natural populations must be maintained in additional ways such as through structured
134 population growth and spatial distribution patterns (Buttery *et al.* 2012; smith *et al.* 2016).
135
136 Despite the great deal has been learned about cooperation and conflict in *D. discoideum,* much
137 remains to be learned with respect to the underlying genes and pathways. Several efforts to
138 identify genes underlying cheating phenotypes have been made, often by employing restriction
139 enzyme-mediated integration (REMI) to generate gene knock-out mutant libraries (Kuspa and
140 Loomis 1992). Screening of such REMI mutant libraries has successfully revealed a number of
141 genes involved in cheating phenotypes in *D. discoideum.* Santorelli *et al.* (2008) screened a
142 large REMI mutant library, focusing on facultative cheater genes (by requiring one round of
143 clonal fruiting body development) and identified over 100 genes predicted to cause cheating
144 when lost to mutation. As might be expected for such a large number of loci, the gene ontology
145 terms span a wide diversity of biological processes. Thus far only two of the genes from
146 Santorelli *et al.* (2008) have been characterized including *chtB* (Santorelli *et al.* 2013) and *chtC*
147 (Khare and Shaulsky 2010). Despite the expectation that mutations in genes that cause cheating
148 should have an associated fitness cost to control their spread, neither the *chtB* nor *chtC*
149 mutants have any obvious fitness costs. Mutant clones for both genes are able to cheat
150 facultatively, increasing in numbers in chimera but when alone, they contribute cells to both
151 spores and stalk and form fruiting bodies normally (Khare and Shaulsky 2010; Santorelli *et al.*
152 2013). It may be that there are disadvantageous pleiotropic effects that keep these mutations
153 from spreading, but they were not detected in the laboratory. Pleiotropy is, after all, another
154 mechanism proposed to hinder the spread of cheaters such as described for two separately

155 identified facultative cheater genes in *D. discoideum*, *dimA* and *csaA* (Queller *et al.* 2003; Foster
156 *et al.* 2004; Strassmann and Queller 2011).
157
158 In addition to the aforementioned facultative cheater genes, only one obligate cheater gene
159 has been described, *fbxA* (Ennis *et al.* 2000). The *fbxA* mutant, also resulting from a REMI
160 mutant library screen, was the first cheater gene to be described and has therefore also been
161 referred to as "Cheater A" or "chtA" for short. When cells from a clone carrying a mutant copy
162 of *fbxA* (encoding F-box protein A) are mixed with wild-type cells, they become
163 overrepresented as spores rather than stalk cells (Ennis *et al.* 2003). But unlike the facultative
164 cheaters, there is a large group cost; as the frequency of *fbxA* mutants in a group increases, the
165 overall spore production decreases (Gilbert *et al.* 2007). And when alone (*i.e.,* only *fbxA*
166 mutants are present), few to no spores are produced; the loss of *fbxA* results in non-fruiting
167 obligate cheaters (Ennis *et al.* 2000, 2003).
168
169 The cheater genes that have been described thus far in *D. discoideum* share few sequence
170 features or protein domains and are associated with a wide diversity of cellular functions and
171 pathways, which suggests that cheating can be accomplished in many ways (Santorelli *et al.*
172 2008). Some of the mechanistic diversity is already apparent; the described cheater genes
173 cause cheating via different means including altered communications in cell-fate determination
174 (Ennis *et al.* 2000; Thompson *et al.* 2004; Khare and Shaulsky 2010) and changes in cell
175 adhesion (Queller *et al.* 2003). Perhaps that is to be expected given the complexity of
176 multicellular development in *D. discoideum*. In addition to the aggregation and cooperation

177 required of the previously free-living individuals, multicellular development involves the
178 differentiation of cell types (*e.g.,* prestalk, prespore), followed by the maintenance and
179 coordination of each of those cell types fates and their proportions (Loomis 2015). Cheaters can
180 presumably arise that exploit any number of aspects of this developmental process; the study
181 of cheating therefore also has the potential to provide insight into development more broadly.
182
183 To expand our understanding of the genomics underlying cheating and cooperation in *D.*
184 *discoideum,* and especially the understudied obligate cheaters, in this study we return to cell
185 lines experimentally evolved under low-relatedness by Kuzdzal-Fick *et al.* (2011). Starting from
186 a single isolate of the wild type lab strain AX4, Kuzdzal-Fick *et al.* (2011) established 24 replicate
187 lines and maintained low-relatedness by transferring a million spores to new plates 31 times
188 (about 290 generations) (**Figure 1A**). Each round began with one million spores which were
189 allowed to hatch, proliferate by eating bacteria, and then form fruiting bodies. At each transfer,
190 the low relatedness was reestablished by replating a million thoroughly mixed spores. In this
191 way, cheaters that appeared by mutation would not be with other such cells among the million
192 and would instead be in close proximity to cells to exploit. Under these conditions, cheaters
193 were favored by selection and significantly increased in abundance by contributing more to
194 spores while contributing less to the stalk. As the percentage of cheaters in a line increased,
195 fewer spores were produced overall. And among the evolved lines, the percentage of clonal
196 isolates which had completely lost cooperation and could no longer form fruiting bodies on
197 their own (non-fruiters) rose to as high as 69% (**Figure 2**). On average, the evolved lines of

198 Kuzdzal-Fick *et al.* (2011) contained approximately 30% non-fruiters and most of them that
199 have been tested were cheaters.
200
201 The work by Kuzdzal-Fick *et al.* (2011) showed that drastically reduced relatedness allowed the
202 spread of cheater mutations that contribute disproportionately to spores and reduced the
203 overall spore production in many lines (**Figure 1A**). This demonstrates how low relatedness in a
204 natural population would lead to a collapse of multicellularity and with it, the advantages of
205 fruiting body formation and spore dispersal. In this study we use whole-genome sequencing
206 and variant analysis of these experimentally evolved *D. discoideum* cell lines to identify genomic
207 changes that allowed non-fruiting obligate cheaters to evolve over the course of that
208 experiment.
209

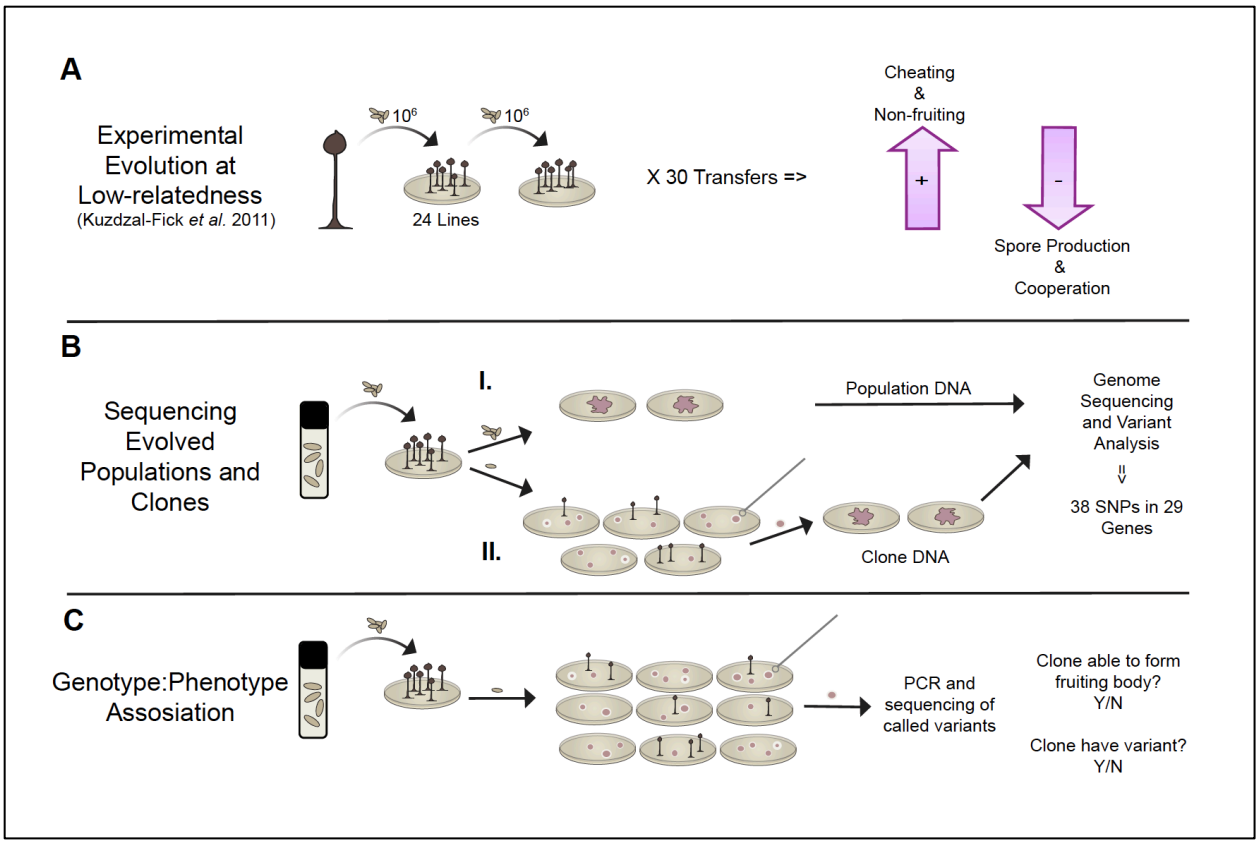


**Figure 1. Outline of the experimental workflow. A.** Experimental evolution of *D. discoideum* at low-relatedness by Kuzdzal-Fick *et al.* (2011). A clonal isolate of AX4 was used to generate 24 replicate lines. After fruiting body formation, spores were collected, thoroughly mixed and one million spores were replated. Reestablishing low relatedness at each of the 31 passages (about 290 generations) allowed selection to favor mutations that conferred cheating. **B.** Whole-genome sequencing and variant analysis in this study of the 24 evolved cell lines (from A). We grew spores from the final passage of each evolved cell line to generate two samples, (**I.**) the line in bulk, as a population and (**II.**) a non-fruiting clone from each line. For the line in bulk as a population (**B, I.**), we grew cells for genomic DNA extraction. For the non-fruiting clone (**B, II.**), we plated a serial dilution of spores from each population to isolate a non-fruiting clone which we then grew for genomic DNA extraction. We used whole-genome sequencing and variant

222 analysis of populations and clones to identify 38 SNPs impacting 29 genes. **C.** Association of
223 SNPs with the loss of altruism in clones. We again plated the evolved populations (lines) (from
224 A) to allow growth of clonal colonies from individual spores. We evaluated numerous clones
225 from each line by two criteria: 1) whether they were obligate cheaters (non-fruiters) or not
226 (normal fruiting body formation) and 2) whether they carried the previously identified SNP or
227 not, via PCR and Sanger sequencing.
228
229
230 **Materials and Methods**
231 ***Experimental Cell Lines***
232 *Dictyostelium discoideum* cell lines were experimentally evolved under conditions of low-
233 relatedness by Kuzdzal-Fick *et al.* (2011) (**Figure 1A**). Kuzdzal-Fick *et al.* (2011) froze spores from
234 the evolved lines in KK2 buffer (2.25 g $KH_2HPO_4$ and 0.67 g $K_2HPO_4$ per L) with 25% glycerol and
235 stored them at -80°. We thawed spores from the ancestor and from the final passage of each
236 evolved line for genomic DNA extraction. Each evolved line is a population composed of cells
237 and lineages carrying any newly acquired mutations. To capture all of this variation, we
238 generated a whole-genome sequence for each evolved line. We will refer to these sequences as
239 populations. To narrow the focus to variation associated with obligate cheating, we also
240 generated a whole-genome sequence for one non-fruiting clone from each evolved line (**Figure**
241 **1B**). We will refer to these sequences as non-fruiter clones. And finally, to identify variation that
242 arose during the experimental evolution we generated a whole-genome sequence of the
243 ancestor.

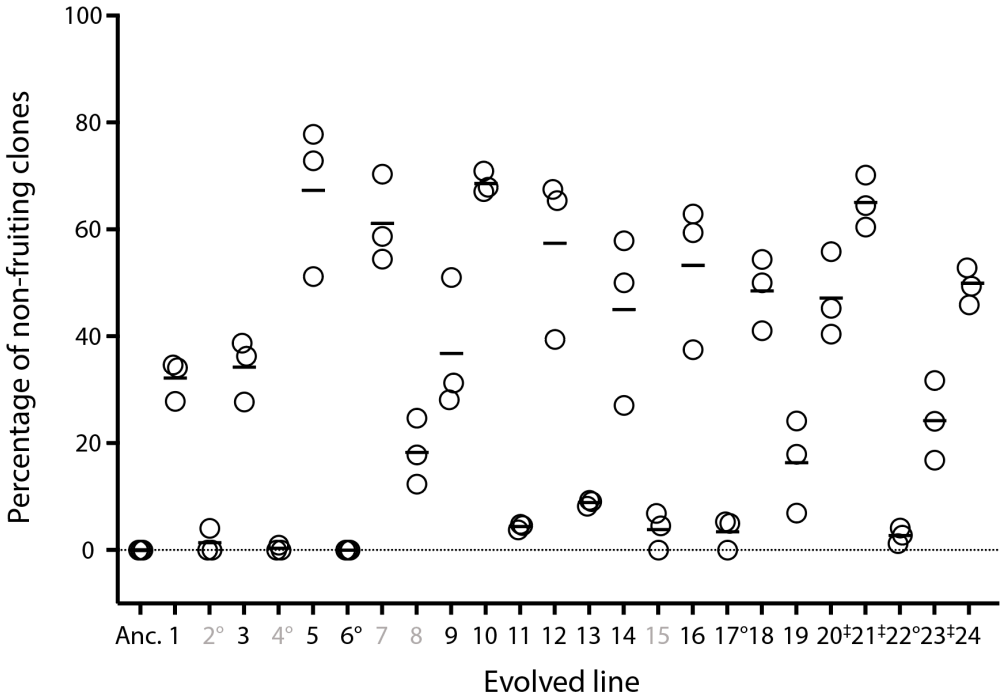


**Figure 2. Percentage of non-fruiting clones per evolved cell line from Kuzdzal-Fick *et al.* (2011).** After about 290 generations under low-relatedness, 19 of the 24 lines had evolved to cheat their ancestor (the five lines that did not cheat are labeled in grey). Non-fruiting (obligate cheating), which was not present in the ancestor (Anc.), also increased in frequency to a varying degree among the evolved lines. The percentage of non-fruiting clones for each line (three replicate measurements) is displayed in this scattered dot plot with the mean represented by the horizontal bar. In this study we generated a whole-genome sequence for each evolved line in bulk as a population and for one non-fruiting clone except where indicated ('°' indicates no clone was sequenced and '‡' indicates two clones sequenced). Redrawn from Kuzdzal-Fick *et al.* (2011).

257

258 To isolate genomic DNA from each of the 24 evolved lines (**Figure 1B, I.**), we plated spores onto
259 two SM/5 agar plates (2 g glucose, 2 g BactoPeptone (Oxoid), 2 g yeast extract (Oxoid), 0.2 g
260 $MgCl_2$, 1.9 g $KH_2PO_4$, 1 g $K_2HPO_4$ and 15 g agar per liter) with 200 µL of *Klebsiella pneumoniae* in
261 KK2 buffer ($OD_{600}$ 1.5) as food. We plated the spores at two different concentrations (2 X $10^5$
262 spores and 4 X $10^5$ spores per plate) to allow processing of multiple samples at one time in case
263 growth rates varied between the evolved lines. We incubated the plates at room temperature
264 for approximately 36 h or until log phase. We collected amoebae in log phase from the surface
265 of two plates for each sample and washed them four to five times in chilled KK2 buffer before
266 DNA extraction.

267

268 To isolate genomic DNA from non-fruiting clones (**Figure 1B, II.**) we first plated serial dilutions
269 of spores to allow for clonal growth from individual spores. We aimed to collect one non-
270 fruiting clone from each evolved line but for five lines (2, 4, 6 and 17 and 22), despite repeated
271 attempts, we were unable to locate any non-fruiting clones. To use the remaining sequencing
272 space, we sequenced a second non-fruiting clone for three haphazardly selected lines (20, 21
273 and 23). After three to five days of growth, we collected cells from the leading edge of each
274 non-fruiting clonal plaque using a sterile loop and plated them on SM/5 agar with *K.*
275 *pneumoniae*. We then plated these cells to grow for DNA extraction using the same protocol
276 described for the evolved lines. To document the non-fruiting morphology, we took
277 photographs of each clonal plaque immediately before collecting cells from the leading edge for
278 expansion (example images are available in **Supplemental Material 1**). A second photograph

279 was taken one to two days following collection and we continued to monitor the plaques to
280 ensure they never formed fruiting bodies.
281
282
283 ***DNA isolation and sequencing***
284 We isolated genomic DNA from the washed, log-phase cells in the range of 1–2 X $10^8$ cells using
285 the Qiagen DNeasy® Blood and Tissue kit (Qiagen). We resuspended the genomic DNA in 10
286 mM Tris-HCl pH 8.5 and stored it at 4° until submission to the McDonnell Genome Institute at
287 Washington University in St. Louis, MO for library preparation and sequencing. Sequence
288 libraries were prepared starting with 0.5 μg of genomic DNA using the KAPA Hyper Library Prep
289 (KAPA Biosystems). We sequenced genomic DNA on the Illumina NovaSeq (150 bp x 2 paired-
290 end) to an estimated depth of 100X and 500X for the clones and populations, respectively.
291
292
293 ***Sequence Alignment***
294 We aligned the Illumina paired-end reads to a single FASTA file containing the reference
295 genomes of both *D. discoideum* AX4 and the food bacterium, *K. pneumoniae* (both downloaded
296 from NCBI in June 2019). We used BWA-MEM (0.7.15) (Li 2013) to index the *D. discoideum* and
297 *K. pneumoniae* concatenated reference genome and to align the paired-end reads for each
298 sample.
299

300 We used an alignment pipeline to run BWA-MEM (Li and Durbin 2009) which converts, sorts
301 and indexes input, intermediate, and output formats using Picard v2.18.1
302 (http://broadinstitute.github.io/picard/), Sambamba v0.6.4 (Tarasov *et al.* 2015) and Samtools
303 v1.3.1 (using HTSLib v1.3.2) (Li *et al.* 2009) ultimately resulting in an aligned, sorted,
304 compressed and indexed CRAM file. We used both Picard (CollectInsertSizeMetrics,
305 CollectAlignmentSummaryMetrics, CollectGcBiasmetrics) and Samtools (flagstat) to evaluate
306 alignment and coverage metrics using BAMs of the initial alignments including both *D.*
307 *discoideum* and *K. pneumoniae* reference genome alignments and again after excluding reads
308 that aligned to *K. pneumoniae*.
309
310
311 ***Variant Calling and Filtration with GATK***
312 We calculated the initial genotype likelihoods using GATK (4.1.2) (McKenna *et al.* 2010)
313 HaplotypeCaller (-ERC GVCF --sample-ploidy 1) for each sample. Next, we ran GATK
314 GenotypeGVCFs (--sample-ploidy 1) to create per-sample genotypes as individual VCF files for
315 the entire *D. discoideum* and *K. pneumoniae* concatenated reference genome. We selected the
316 *D. discoideum* chromosomes (and the unplaced contigs associated with the reference genome)
317 from the VCF files for downstream annotation and filtering using GATK SelectVariants. We used
318 the Ensembl Variant Effect Predictor (VEP 95.3) (McLaren *et al.* 2016) to annotate all variants
319 and add sequence ontology terms (--term SO) using the dicty2.7 assembly of
320 '*Dictyostelium_discoideum*' from Ensembl Protists (release 43). We decomposed complex
321 variants using vt decompose (Tan *et al.* 2015) before adding allele frequencies, merging or

322 filtering. We then processed the decomposed variants with bam-readcount (0.7.4)
323 (https://github.com/genome/bam-readcount) and cyvcf2 (https://github.com/brentp/cyvcf2)
324 to generate allele frequencies. We used VAtools (https://github.com/griffithlab/VAtools, 3.1.0)
325 to add the AF (allele frequency) format fields to each sample including the allele frequencies of
326 each allele as calculated by bam-readcount allele counts. We processed all per-sample VCFs
327 with bgzip and tabix for speed and storage before merging to generate the full per-sample call
328 set VCF using GATK (3.6) CombineVariants (-genotypeMergeOptions UNIQUIFY).
329
330 We performed variant filtration of the GATK VCF using bcftools v1.12 (using HTSLib v1.12) (Li
331 2011) and GATK. We did not consider indels or sites with more than one alternate allele. We
332 are only interested in variation that arose during the course of experimental evolution or, new
333 variation between the ancestor and the evolved lines. To exclude pre-existing variation we first
334 removed sites (from all samples) for which the ancestor was called as a variant (*i.e.,* sites in the
335 ancestor that differed from the reference genome) as well as sites that were left uncalled in the
336 ancestor. To remove ancestral polymorphism we next calculated the major allele frequency
337 (MAF) of all sites in the ancestor BAM file using bam-readcount (0.7.4)
338 (https://github.com/genome/bam-readcount). Using that information, we then removed sites
339 (from all samples) for which in the ancestor, the MAF < 0.90.
340
341 We applied hard filters using GATK VariantFiltration and SelectVariants following the GATK Best
342 Practices standard recommendations (QD > 2, FS < 60, SOR < 3, MQ > 40, MQRankSum > -12.5
343 and ReadPosRankSum > -8). Next we applied custom filters using bcftools view. The first custom

344 filter was the removal of sites missing too much data, which we defined as sites left uncalled in
345 more than 10 samples. For each of the 24 evolved lines we sequenced the whole line (as a
346 population), and for most of the lines we also sequenced one non-fruiting clone, for a total of
347 two samples per line (or a total of three samples for lines 20, 21 and 23 for which we
348 sequenced two clones). There is a low likelihood that the same SNP will occur by chance in
349 more than one evolved line. But because we sequenced two or three samples for each line (the
350 population and individual clones) the maximum number of times that a SNP is likely to appear
351 in our data is twice (or three times for lines 20, 21 and 23). For this reason, we applied a
352 maximum alternate allele count (AC) of three. Next, we applied a minimum Phred-based quality
353 score (QUAL) of 200 to remove low-quality sites and we removed sites with more than 1.5
354 times the average approximate read depth (DP) to reduce false positives. Last, we manually
355 reviewed this final set of SNPs using the Integrative Genomics Viewer (IGV) to further reduce
356 the number of false positives and misclassifications (Robinson *et al.* 2011, 2017).
357
358
359 ***Variant Calling and Filtration with Freebayes***
360 We also performed joint variant calling on all samples using Freebayes v1.3.1-dirty (Garrison
361 and Marth 2012). We used the default parameters but for the following exceptions: sample
362 ploidy of one, pooled continuous mode, minimum base quality 10, minimum mapping quality
363 10 and we only retained the best of six alleles. We streamed variant calls directly through the
364 vcflib (Garrison *et al.* 2021) vcffilter, to remove variants with a quality score below 20. We

365 decomposed complex variants into their constituent SNPs and indels using vcflib
366 vcfallelicprimitives followed by normalization with vt (Tan *et al.* 2015).
367
368 We performed variant filtration of the normalized Freebayes VCF using bcftools v1.12 (using
369 HTSLib v1.12) (Li 2011) following a similar process to that used for filtering the GATK VCF.
370 Although the two callers calculate and output some different metrics for quality assessment,
371 we generated filters resembling those applied to the GATK VCF as much as possible. First, we
372 excluded indels and sites with more than one alternate allele, followed by the removal of
373 background variation as described for the GATK VCF (ancestral sites with an MAF < 0.90 or sites
374 in the ancestor that were either called as a variant or left uncalled). Next we applied hard filters
375 to remove calls affected by mapping quality or strand bias (MQM > 40, SAF > 0 and SAR > 0, SAP
376 > 0.5 and SRP > 0.5, RPR > 1 and RPL > 1). We then applied the same set of custom filters to the
377 Freebayes VCF as described for the GATK VCF including the removal of sites with more than 10
378 missing samples, sites with an alternate allele count (AC) greater than three and sites with a
379 Phred-based quality score (QUAL) below 200. Finally, based on the approximate read depth
380 (DP) in this remaining set of variants we removed sites with more than 1.5 times the average to
381 reduce false positives. To further reduce the number of false positives and misclassifications we
382 manually reviewed this final set of SNPs using the Integrative Genomics Viewer (IGV) (Robinson
383 *et al.* 2011, 2017).
384
385 ***The Intersection of GATK and Freebayes VCFs and Variant Read Support***

386 We viewed the two separately generated and filtered VCF files (from GATK and Freebayes) side-
387 by-side and removed four sites that were not present in both files. The SNPs we removed
388 included one SNP that had only been initially called by one of the callers and three SNPs that
389 although initially called by both callers, only survived the filtration in one of the separate
390 filtering pipelines. Going forward we worked with these cross-validated SNPs in the annotated
391 GATK generated VCF.
392
393 As one final verification of variant support and quality we confirmed that each variant that had
394 been called in a non-fruiting clone could also be detected in its origin population (or the line
395 from which the clone was isolated). To do this, we generated read counts for each SNP across
396 all samples using bam-readcount v0.7.4 (https://github.com/genome/bam-readcount). We
397 removed any SNP for which the origin population did not support the same alternate allele with
398 at least five reads, which we expect would only occur for false positives or for SNPs that did not
399 provide a selective advantage. Also, because we expect that most true variants will be unique
400 to one replicate line, for each SNP we viewed the number of reads supporting the same
401 alternate allele across all samples. This led to the removal of one SNP that shared low level
402 support for the same allele across multiple lines and also the rejection of one sample from a
403 variant call (for details see *Variant Read Support* in the **Supplemental Methods**).
404
405
406 ***Functional Annotation Clustering of Genes with SNPs***

407 We performed functional annotation enrichment analysis with the final set of 29 genes
408 containing SNPs using the online tool, DAVID (Database for Annotation, Visualization and
409 Integrated Discovery (https://david.ncifcrf.gov/; Huang *et al.* 2009a, 2009b). We determined
410 enriched terms using a Benjamini-corrected p-value (< 0.05) (Benjamini and Hochberg 1995).
411
412
413 ***Structural Variant (SV) Calling and Filtration with Delly***
414 We called structural variants (SVs) with Delly v0.8.3 (Rausch *et al.* 2012) following the Germline
415 SV Calling workflow. We first did per-sample SV calling, providing the indexed, sorted and
416 duplicate-marked BAM files and the indexed *D. discoideum* and *K. pneumoniae* concatenated
417 reference genome. We then merged the SV sites to a single list and called genotypes across all
418 samples. We merged all samples genotypes using bcftools v1.12 (using HTSLib v1.12) (Li 2011).
419 We applied the Delly filter (-f germline) and then removed low quality variants that were not
420 flagged as "PASS" in the VCF filter field (PE > 3 [or PE > 5 for translocations] and QUAL >=20).
421 We annotated the SVs using the Ensembl Variant Effect Predictor (VEP 95.3) as described for
422 the GATK VCF. We only retained simple, intrachromosomal SVs. As described for the SNPs, the
423 same SV is unlikely to occur in more than one evolved line. But because we sequenced two or
424 three samples for each line (the population and individual clones) the maximum number of
425 times that a SNP is likely to appear in our data is twice (or three times for lines 20, 21 and 23).
426 For this reason, we discarded SVs that were called in more than three samples. Last, as
427 described for the SNPs, we manually reviewed this final set of SVs in IGV (Robinson *et al.* 2011).
428

429

430 ***Association of Variants with the Loss of Altruism***

431 To investigate for a potential correlation between variants and the complete loss of
432 cooperation we returned to some of the evolved lines to isolate additional clones for targeted
433 re-sequencing (**Figure 1C**). Each evolved line is a population comprised of both cooperators and
434 evolved cheaters. The complete loss of cooperation is therefore only revealed when spores are
435 plated clonally and can be identified by an inability to form a fruiting body (non-fruiting clones).
436 Taking advantage of this population variation (**Figure 2**) we scored multiple additional clones
437 for 1) whether or not it was able to form a fruiting body in isolation and 2) the presence or
438 absence of the called variant(s) in the line.

439

440 For this analysis we again plated the evolved cell lines clonally (as described in the section,
441 *Experimental Cell Lines*) to allow for growth from individual spores. After three to five days of
442 growth we screened clones via PCR and Sanger sequencing. As previously described (in the
443 section, *Experimental Cell Lines*), we took photographs of the screened clones to document the
444 presence or absence of fruiting body formation (example images are available in **Supplemental**
445 **Material 1**).

446

447 We generated genomic DNA for PCR genotyping clones using one of two methods. For some of
448 the clones we first collected cells from the leading edge of the plaque, grew them to larger
449 numbers and carried out a formal DNA extraction with the DNeasy® Blood and Tissue kit
450 (Qiagen). To increase throughput, for most clones we directly lysed cells from the leading edge

451 of the plaque and used the lysate for what we called a "plaque PCR." Based on a protocol
452 described by Charette and Cosson (2004), the plaque PCR included two steps. First, we used a
453 sterile pipette tip to collect a small number of cells from the leading edge of a plaque and
454 placed it in a tube containing 20 µl lysis buffer (10 mM Tris, pH 8.3, 50 mM KCl, 2.5 mM $MgCl_2$,
455 0.45% Nonidet® P-40 (NP40) and 0.45% Tween® 20) with PK (1 µL of 20 µg/µL of PK for every 25
456 µL of lysis buffer). Next, we incubated the cells in lysis buffer for 1 min at 95° to inactivate the
457 PK after which we used the cell lysate for PCR or stored them at -20°.
458
459 We designed primers to PCR-amplify the region spanning each called variant of interest
460 (**Supplemental Table S1**). For the PCR we used either 1 µl of cell lysate or approximately 10 ng
461 of DNA for the formal DNA isolations and the following reaction components: $MgCl_2$ (25 mM) 1
462 µl, dNTPs (10 mM each) 0.5 µl, 5 pM of each primer, 5X GoTaq® Flexi Buffer 5 µl, GoTaq® DNA
463 Polymerase 0.2 µl and $H_20$ 10.3 µl for a 20 µl reaction. We used the following PCR protocol
464 (adjusting the annealing temperature as needed, according to primer pairing): 95°, 2:00; 95°,
465 0:15; 50°, 0:15; 60°, 3:00; repeat steps 2–4 34X, 60°, 5:00; 4° hold. We submitted PCR products
466 and primers (the same primers used for amplification) to Genewiz (South Plainfield, NJ) for
467 purification and Sanger sequencing. We trimmed the returned sequences with 4Peaks
468 (https://nucleobytes.com/4peaks/) for alignment using Seaview
469 (http://doua.prabi.fr/software/seaview).
470
471 We screened a varying number of clones according to the availability of the fruiting and non-
472 fruiting clones from each line. For each line included in this screen we tallied the number of

473 clones that did and did not carry the called mutation(s) and whether or not the clone was able
474 to form a fruiting body when plated clonally. We tested for significance using Fisher's Exact Test
475 with a 95% confidence interval using GraphPad Prism (version 9.3 for MacOS).
476
477
478 ***Predicted Protein Structure***
479 To explore proteins of interest, we first downloaded the amino acid sequences from DictyBase
480 (Fey *et al.* 2009) and submitted them to Protter (Omasits *et al.* 2014) for visualization. We
481 accessed three-dimensional structural predictions generated by AlphaFold
482 (https://alphafold.ebi.ac.uk/) (Jumper *et al.* 2021; Varadi *et al.* 2022).
483
484
485 ***Data Availability Statement***
486 Raw reads in CRAM format will be stored in the Sequence Read Archive (SRA) [link/citation]
487 (accession numbers/DOIs). Variant calls that survived filtration from each of the three variant
488 callers (GATK, Freebayes and Delly) are available in **Supplemental Material 2** in VCF format. All
489 cell lines used in this study are in the lab of the senior authors and are available upon request.
490
491
492 **Results**
493 ***Raw Data Generation and Alignment***

494 We obtained over 5 trillion reads across all samples, with a high rate of alignment (94.7%) to
495 the concatenated *D. discoideum* and *K. pneumoniae* reference genomes. All reads that aligned
496 to *K. pneumoniae* (food bacterium) were excluded from further analysis. The remaining 2.7
497 trillion reads aligned to *D. discoideum* with an average rate of 89.3%. Read alignment was, on
498 average, equally successful for clones and evolved lines (89.3% and 89.4%, respectively). The
499 average mapped read depth of all annotated genes normalized by gene length (gene
500 annotations downloaded from NCBI on 10-25-19, **Supplemental Material 3)** is 54X and 195X for
501 clones and evolved lines, respectively (**Table 1**). The average mapped read depth of normalized
502 intergenic regions is very similar with averages of 53X and 180X for clones and evolved lines,
503 respectively.
504
505
506 ***Resulting SNPs are Selection Driven***
507 We joint called SNPs across all samples resulting in 53,220 unfiltered variants with GATK and
508 32,775 with Freebayes (before normalization). After independently filtering each call set the
509 GATK VCF contained 306 SNPs and the Freebayes VCF contained 230 SNPs (the number of
510 variants removed by each filter is available in **Supplemental Material 4**). We next manually
511 reviewed all remaining SNPs in IGV resulting in approximatly 75 sites in each call set. Finally, we
512 removed any sites that did not co-occur in both call sets and/or sites lacking read support (as
513 described in ***The Intersection of GATK and Freebayes VCFs and Variant Read Support***). The
514 final set of SNPs contained 38 biallelic SNPs associated with 29 different genes (**Table 2**). Each
515 gene in this list has only one SNP except for the gene, *grlG* (DDB_G0272244), which has 10

516 unique SNPs (discussed in detail in the following sections). All SNPs are unique to one evolved
517 line with the exception of one in the unannotated gene, DDB_G0276529, which was called in
518 two lines (7 and 16). Most evolved lines have between one and three SNPs except for lines 7
519 and 21, which have five and eight SNPs each, respectively (**Table 1**).
520
521 Most SNPs (31 of 38) are in coding regions of the genome and all but one of these result in an
522 introduced stop codon or amino acid substitution (**Table 2**). Among the 31 SNPs in coding
523 sequence, 22 are missense variants and according to the Variant Effect Predictor annotations
524 are predicted to have a moderate impact, eight others introduce a premature stop codon with
525 a high predicted impact and the one synonymous variant has a low predicted impact. Among
526 the seven SNPs in non-coding sequence, five are upstream and two are downstream variants
527 that the Variant Effect Predictor annotated as "modifier," meaning they are either difficult to
528 predict or that there is no evidence of an impact. This distribution of large effect SNPs strongly
529 supports that they have increased in abundance due to selection, rather than drift.
530
531
532 ***Genes with SNPs***
533 The 29 genes with SNPs (**Table 2**) are distributed throughout the *D. discoideum* genome with
534 between one and eight SNPs on each of the six chromosomes. The average GC for the set of 29
535 genes (excluding introns) is 28.4% which is close to the genome-wide average of 27% for
536 protein-coding genes. Each of the genes in our list has one SNP except for the G protein-
537 coupled receptor (GPCR), *grlG*, which has 10 unique SNPs. *GrlG* is one of 17 glutamate receptor-

538 like ('grl') proteins in the *D. discoideum* genome (*grlA*–H and *grlJ*–R) (Eichinger *et al.* 2005) but
539 the function of *grlG* is not yet known. And like the majority of glutamate receptor-like proteins
540 in *D. discoideum*, we do not know the ligand(s) that it binds nor the downstream effector(s).
541 Among the remaining 28 genes (each with one unique SNP) a few have been well described
542 (*e.g., sgmA*, *pks39* and *arkA*) but the majority (17) are hypothetical proteins still largely lacking
543 annotation.
544
545 Using annotations that are available for our 29 genes with SNPs, we carried out functional
546 annotation clustering with DAVID and identified two significantly enriched annotation clusters.
547 The first cluster of five annotations contained UniProt Keywords (Bateman *et al.* 2021) related
548 to zinc and metal binding (group enrichment score of 1.45) including *arkA*, DDB_G0272484,
549 *rnf160*, DDB_G0269332 and *sgmA*. The second cluster of 10 annotations contained terms
550 related to transmembrane and membrane annotations (group enrichment score of 1.11). This
551 second cluster contained *arkA* and DDB_G0269332 from the first cluster as well as *grlG*, *pks39*,
552 DDB_G0276291, DDB_G0278531, DDB_G0278575, DDB_G0281923, DDB_G0290523 and
553 *tmem144A*. After applying the Benjamini (Benjamini and Hochberg 1995) correction, none of
554 the individual terms are significantly enriched (**Supplemental Material 5**). The large number of
555 unannotated genes implicated here does hinder interpretation, but it is not unusual given that
556 at the time of writing this manuscript, approximately 40% of protein-coding genes in the *D.*
557 *discoideum* genome still lack annotation (Fey *et al.* 2009).
558
559

560 ***Structural Variants (SVs) Provide Further Support for grlG***

561 We joint called structural variants (SVs) across all samples using Delly resulting in an unfiltered
562 set of 10,139 SVs. The Delly filter reduced the number to 131 and after all quality filtration we
563 have a set of 12 SVs (**Supplemental Table S2**). Among the 12 SVs are six deletions, five
564 inversions and one duplication. Nine of the 24 evolved lines carry 1 or more of these SVs, two of
565 which (lines 1 and 14) did not have any called SNPs. Each SV is unique to one evolved line with
566 the exception of one deletion (NC_007088.5:1742215–1742506) in *grlG* which was called in
567 lines 17 and 18. However, because we cannot rule out potential contamination of the
568 population sample of line 18 we only report the variant in line 17 (more detail is available in
569 *Variant Read Support* in the **Supplemental Methods**). The deletion was verified by PCR in line
570 17 (as part of the analysis described in the section, *Association of Variants with the Loss of*
571 *Altruism*). The SVs range considerably in length (from 183 bp to 49 Kb) potentially impacting as
572 many as 21 different genes. Strikingly, five of the 12 SVs impact *grlG*, the same gene that we
573 already identified as carrying 10 SNPs. None of the 28 other genes with SNPs were impacted by
574 any of the SVs. Given the clear signals of parallel evolution identified for *grlG*, we chose not to
575 pursue the other SVs any further. We will only discuss the SVs that impact *grlG* going forward;
576 the full set of 29 SVs that passed filtration are available in VCF format in **Supplemental Material**
577 **2**.

578

579

580 ***Some Variants in grlG are Associated with the Loss of Cooperation***

581 Given the high level of parallelism identified in *grlG* (one or more variants in more than half of
582 the evolved lines) we returned to the evolved lines to screen additional fruiting and non-fruiting
583 clones for a correlation between variants in *grlG* and the loss of cooperation. The variants are
584 located throughout the length of the gene but a pattern emerged in which only those variants
585 located in the 5' half of *grlG* (on exon 1) are associated with the loss of cooperation (*i.e.,* non-
586 fruiting clones) and variants in the 3' half (on exon 2) are not (**Figure 3** and **Supplemental Table**
587 **S3**). Because *grlG* has two exons of roughly equal length (383 and 390 amino acids for exon 1
588 and exon2, respectively) and for simplicity, we will refer to the two halves as the 5' and 3'
589 regions.
590
591 We prioritized screening of variants that we had identified in evolved lines with a moderate
592 percentage of non-fruiting clones (**Figure 2**) so that both fruiting and non-fruiting clones could
593 be included. We also prioritized variants with moderate allele frequencies in their evolved
594 populations. As such, the analysis included ten of the 15 variants identified across the length of
595 *grlG*. The 10 variants were called in 8 different lines (two unique variants were called in lines 21
596 and 17), three of which have variants in the 5' region (lines 5, 21 and 24) and five with variants
597 in the 3' region (7, 10, 11, 13 and 17). From the three lines with variants in the 5' region, we
598 screened 88 clones (62 non-fruiters and 27 fruiters) for the presence of four called variants. We
599 found that 88.7% (55 of 62) of the non-fruiter clones carried the variant compared to only 3.7%
600 (1 of 27) of the fruiting clones. The association between the presence of variants in the 5'
601 region of *grlG* and the clonal phenotype is significant in each evolved line we screened (Fisher's
602 Exact $p < 0.0001$, $p = 0.0164$ and $p < 0.0001$ for lines 5, 21 and 24, respectively). In the 3' region,

603 from the five lines with variants, we screened 78 clones (39 non-fruiters and 39 fruiters) for the
604 presence of six called variants. Unlike the association in the 5' region, we found the number of
605 clones carrying a variant in the 3' region was roughly equal between non-fruiters and fruiters
606 (94.8% [37 of 39] and 87.2% [34 of 39], respectively). There is no association between the
607 presence of variants in the 3' region of *grlG* and the clonal phenotype in any of the evolved
608 lines we screened (Fisher's Exact $p > 0.05$).
609
610 According to our results, variants in the 5' region of *grlG* are significantly associated with the
611 non-fruiting phenotype but not all clones follow that trend (**Figure 3**). In all three evolved lines
612 that we screened in the 5' region, we found a few clones that did not have a variant, but they
613 were still unable to form fruiting bodies in isolation. These clones could have lost cooperation
614 because of a different, undetected variant (anywhere in the genome). However, a clone that is
615 still able to cooperate and form a fruiting body in isolation, despite the apparent loss of *grlG,* is
616 more difficult to align with our hypothesis that high impact variants in *grlG* cause non-fruiting.
617 We only found one such clone in the 5' region. One clone from line 21 was able to form a
618 fruiting body despite carrying a SNP that introduces a premature stop codon in *grlG* after only
619 23 amino acids. None of the other 26 fruiting clones that we screened in the 5' region carried a
620 variant in *grlG*. This is strikingly different from the results in the 3' region, where almost all of
621 the fruiting clones that we screened carried a variant in *grlG,* though these were concentrated
622 in lines 11 and 17 and rare in others. Thus, variants in the 5’ region of *grlG* usually result in the
623 loss of cooperation but variants in the 3’ region do not. For a subset of the clones that we
624 screened for *grlG* variants we also screened for the presence of one or more SNPs that we

625 called in other gene(s). These additional screens were largely uninformative and are therefore

626 only described in the supplemental materials (**Additional File 1** and **Supplemental Table S4**).

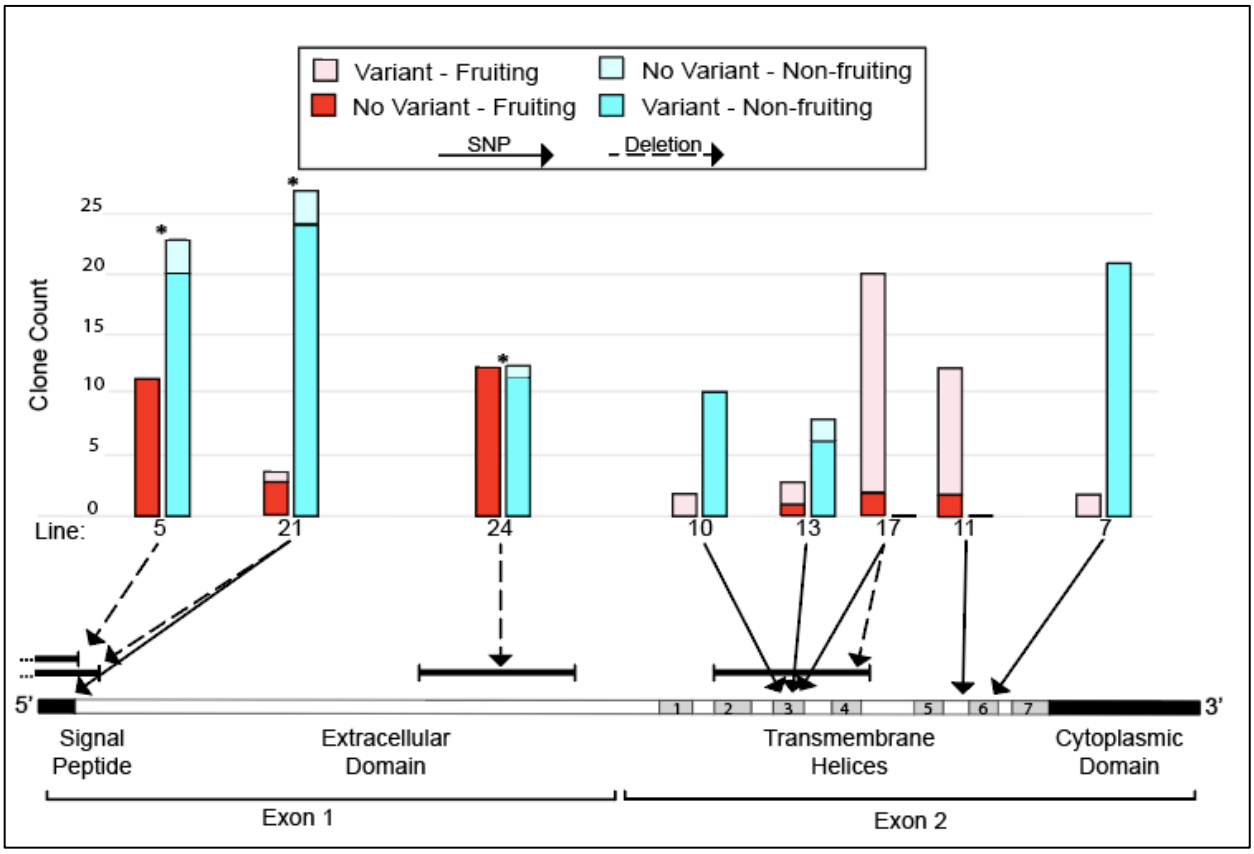


627

628 **Figure 3. Location of variants in *grlG* and correlation with the loss of cooperation.** Schematic

629 representation (drawn to scale) of the coding sequence of *grlG*. The major features of a mature

630 *grlG* protein are indicated below the schematic (see also, **Figure 5).** Ten of the 15 called variants

631 (labeled above the schematic) were included in a targeted resequencing of additional clones

632 from each respective evolved line to investigate the association between variants in *grlG* and

633 the loss of cooperation (clonal inability to form a fruiting body). For each evolved line that we

634 screened clones from, a histogram illustrates the results with side-by-side bars showing the

635 number of clones that could (left bar) and could not (right bar) form a fruiting body in isolation

636 and the number of each phenotype (fruiting or non-fruiting) that did or did not carry the called
637 variant. Significant associations are indicated by an asterisk (*).
638
639
640 ***The Genes Discovered in This Study Have Not Previously Been Implicated in Cheating***
641 To look for a relationship between the 29 genes identified herein and the loss of altruism, we
642 turned to the literature to see if any of them have been previously implicated in cheating in *D.*
643 *discoideum*. Because we are looking for obligate cheater genes, most notably missing from our
644 list is *fbxA,* the only previously known obligate cheater gene (Ennis *et al.* 2000). It is also
645 interesting that our list does not contain any of the characterized facultative cheater genes such
646 as *chtB, chtC*, *dimA* or *csA* (Queller *et al.* 2003; Foster *et al.* 2004; Khare and Shaulsky 2010;
647 Santorelli *et al.* 2013). Aside from that handful of genes that first come to mind, the remaining
648 majority of genes with potential involvement in cheating in *D. discoideum*, have not yet
649 received attention at the individual level. We were particularly interested in the many loci
650 recovered in the large restriction enzyme-mediated insertional (REMI) mutant library screening
651 from Santorelli *et al.* (2008). In that study, a set of 167 mutants (corresponding to 197 loci)
652 were identified that increased under low-relatedness selection. Based on testing a subset of
653 those mutants, the authors estimate that approximately 75% of the mutants are cheaters, but
654 so far, only *chtB* and *chtC* have been described. Although Santorelli *et al.* (2008) focused on
655 facultative cheater genes (by requiring one round of solo fruiting body formation) they did
656 recover *fbxA* and a few other mutants were found with morphological abnormalities indicating
657 there may be a others that are not facultative. The full set of 197 loci identified by Santorelli *et*

658 *al.* (2008) is the first of four gene lists we chose for cross-comparison. The other gene sets are
659 each comprised of genes found to be differentially expressed in chimeric mixtures identified at
660 various stages of multicellular development and thus may contain genes involved in conflict and
661 cheating. Two are comprised of genes identified at tight aggregate stage (79 genes) or the slug
662 stage (190 genes) (Noh *et al.* 2018 and Oliveira *et al.* 2019, respectively). The last gene set is
663 composed of 152 genes that were also identified during the establishment of multicellularity (at
664 either 8 or 12 hours), but in this case, the strains had been engineered to be mutually
665 incompatible (*tgrB1*/*tgrC1* gene replacement strains) which may increase the potential to
666 identify genes involved in conflict (Hirose *et al.* 2015). Unlike the genes from Santorelli et al.
667 (2008) these last three gene sets have not been directly implicated in cheating. But given their
668 differential expression in chimeras, a time at which cheating or the resistance to cheating
669 would be adaptive (Noh *et al.* 2018), they are likely to include genes involved in conflict and
670 cheating. In support of this reasoning, the 79 genes from Noh *et al.* (2018) show signatures of
671 rapid molecular evolution, consistent with conflict driven escalating arms races (Queller and
672 Strassmann 2018; Scott and Queller 2019). For simplicity, we will refer to these four sets of
673 genes as candidate cheater genes.
674
675 Altogether, the four sets of candidate cheater genes from the literature comprise a list of 591
676 unique genes (**Supplemental Table S4**). None of the 29 genes identified in this study were
677 found on that list and there is little overlap among the four candidate cheater gene sets (**Figure**
678 **4**). This in line with previous reports of limited overlap among sets of social genes (kin
679 discrimination, cooperation and cheating) (Oliveira *et al.* 2019; Noh *et al.* 2020). Only 26 of the

591 genes are present on more than one list. No genes are present on all four lists and only one gene is present on three of the four; the pre-spore specific gene D (*pspD*). Because the genes from Santorelli *et al.* (2008) were identified as part of a screen for cheater genes specifically, they are of particular interest. Eleven genes from Santorelli *et al.* (2008) were found on one or more of the other gene lists and three of them were among the subset of mutants directly tested for cheating in that study. One of these tested mutants (LAS92) had an insertion in a gene that is also on the list from Hirose *et al.* (2015) and it was confirmed to be a cheater (DDB_G0283373). Two other tested mutants had intergenic insertions near genes that are also on the list from Oliveira *et al.* (2019); one of which was confirmed to be a cheater (LAS6) (DDB_G0276335) and the other was not (LAS60) (DDB_G0285843). However, these last two mutants from Santorelli *et al.* (2008) had intergenic insertions and the actual gene(s) impacted was not precisely determined.

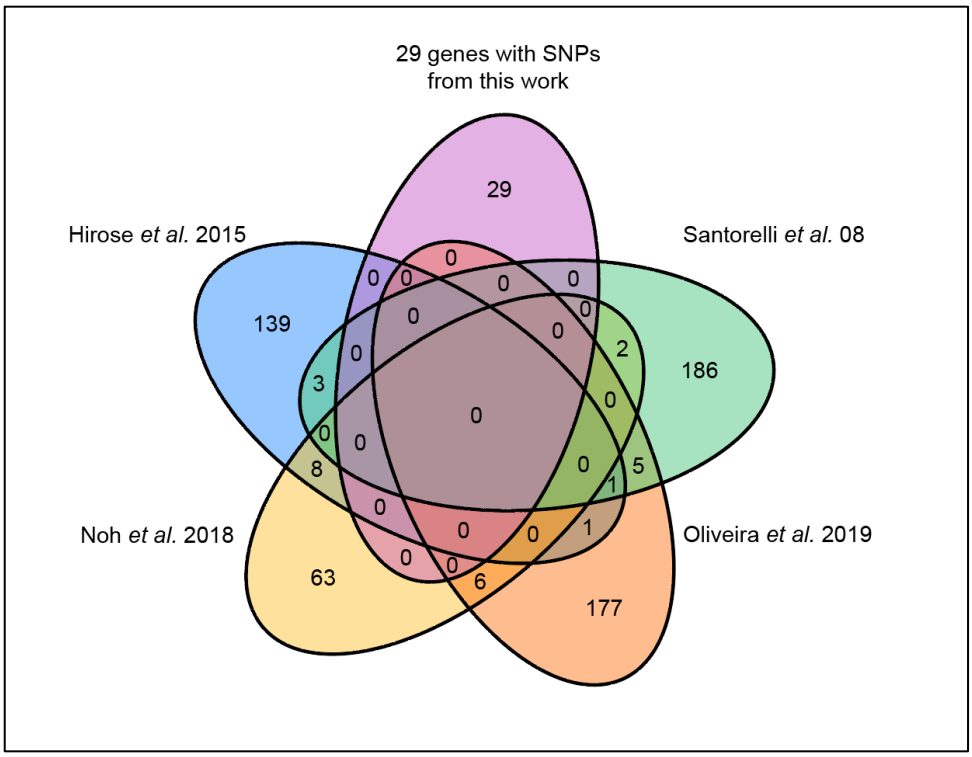
29 genes with SNPs
from this work
29
Hirose et al. 2015
139
Santorelli et al. 08
186
Noh et al. 2018
63
Oliveira et al. 2019
177
0
0
0

706

707 **Discussion**

708 In this study we identified SNPs in 29 genes that arose across 24 replicate lines of *D. discoideum*
709 experimentally evolved by Kuzdzal-Fick *et al.* (2011) under conditions that mean low-
710 relatedness for any new mutations. In that earlier study, over the course of about 290
711 generations at low-relatedness, 19 of the 24 replicate lines saw a significant rise in cheating,
712 defined as a mutant contributing proportionally more to spore cells than stalk cells. When
713 isolates from these lines were plated clonally, an average of 31% had completely lost altruism
714 and were unable to form fruiting bodies on their own. Because each line is a mixed population,
715 the mutations that conferred the obligate cheating advantage were able to spread by forming
716 chimeric fruiting bodies with cooperators lacking the mutation. Here we used whole-genome
717 sequencing and variant analyses of those previously evolved cell lines to identify which genes
718 had changed and might be responsible for the non-fruiting, obligate cheating phenotype. While
719 there are many genes known to cause facultative cheating, before this study only one gene
720 (*fbxA*) had been recognized to cause obligate cheating. We identified at least one SNP in 17 of
721 the 24 experimentally evolved lines for a total of 38 SNPs. Most of the SNPs (31) are in coding
722 regions of the genome, and all but one results in either an introduced stop codon or other
723 amino acid substitution suggesting selective pressure acting on these loci under the
724 experimental conditions in Kuzdzal-Fick *et al.* (2011). The majority of the genes with SNPs are
725 not well characterized and many lack any annotation which impacted our ability to assess any
726 uniting similarities among them. Except for one of these genes, *grlG*, with 10 unique SNPs
727 across multiple lines, the other 28 genes only have one SNP each. *GrlG* also stands out because

728 we found it also harbors five structural variants, whereas none of the other genes with SNPs
729 had any. Our results provide strong evidence of parallel evolution of *grlG* and suggests the
730 involvement of this G protein-coupled receptor (GPCR) in cooperation and multicellular
731 development in *D. discoideum*.
732
733
734 ***Confidence in Variant Calls and Detection***
735 The *D. discoideum* genome has features that may have impacted our ability to detect variants.
736 The AT content of the *D. discoideum* genome is very high, greater than 77% (Eichinger *et al.*
737 2005). The high AT content contributes to the high density of simple sequence repeats (DNA
738 tracts of 1–6 bp tandemly repeated a varying number of times) (Tian *et al.* 2011) which
739 represent 14.3% of the genome (Srivastava *et al.* 2019). Moreover, in *D. discoideum*, these
740 repeats are not confined to non-coding regions; they are also found in over 16.3% of protein
741 coding genes (Eichinger *et al.* 2005). Simple sequence repeats are recognized as mutational
742 hotspots across a number of organisms and are particularly prone to insertions and deletions
743 (indels) (Tóth *et al.* 2000; Ellegren 2004). In *D. discoideum*, both indels and SNPs have been
744 shown to occur at a higher frequency in low-complexity, repetitive regions of the genome
745 (Srivastava *et al.* 2019). The precision of variant calling is also decreased in the same sorts of
746 low-complexity and repeat regions, compounding the challenges of variant calling in *D.*
747 *discoideum*. This decreased precision is particularly true for detection of structural variants,
748 which are inherently more challenging to identify, particularly with short-read sequence data
749 (Cameron *et al.* 2019; Kosugi *et al.* 2019; Mahmoud *et al.* 2019). Despite these challenges, we

750 chose not to exclude low-complexity or non-coding regions of the genome, which could lead to
751 undiscovered variation outright. Instead, we dealt with the challenging features of the *D.*
752 *discoideum* genome by carefully exploring the effects of different settings for variant calling and
753 filtering to determine a stringent and robust pipeline. We separately called SNPs with two
754 independent callers. We applied our carefully chosen quality filters to the two call sets
755 independently, followed by manual inspection of all variants. We then conservatively only
756 pursued the SNPs still present in both call sets. Finally, we used the BAM read counts across all
757 samples to rule out potential contamination or other false positives. Together, despite the
758 challenging features of the *D. discoideum* genome, we are confident that we obtained a high
759 quality and strongly supported set of variants.
760
761 Our stringent pipeline decreased the likelihood of obtaining false positives and ensured that
762 variants called at the population level tend to be those most strongly selected. The trade-off of
763 such a stringent approach is a decreased sensitivity to detect low frequency variants in the
764 population samples. Given the relatively short amount of time the experimental lines were
765 allowed to evolve (Kuzdzal-Fick *et al.* 2011), not all variants would have had the time to expand
766 throughout the population of that line. Therefore, variants that arose later in the experiment or
767 those not facing strong selection, may have been difficult for us to detect at the population
768 level. Although we cannot rule out the possibility that some were left undetected, we did
769 detect some low frequency variants by sequencing individual non-fruiting clones from the lines.
770
771

772 ***Parallel Evolution and the Involvement of grlG in Cooperation***

773 The concentration of highly supported and unique variants in *grlG* across 14 of the 24 replicate
774 lines is strong evidence of parallel evolution at the gene level (Tenaillon *et al.* 2012; Barrick and
775 Lenski 2013; Van den Bergh *et al.* 2018). None of these mutations were present in the ancestral
776 line, indicating that they occurred during the course of experimental evolution (Kuzdzal-Fick *et*
777 *al.* 2011). At the nucleotide level there is no indication of a mutational hotspot because the
778 variants are located throughout the length of the gene. Moreover, the variants in *grlG* are
779 comprised of several types of mutations including 10 non-synonymous SNPs that result in
780 either an introduced stop codon (four) or a missense mutation (six), as well as four deletions
781 and one inversion, all of which impact coding sequence. The number of large-effect mutations
782 (half of which result in protein truncation) and the complete lack of synonymous mutations in
783 *grlG* suggests that the loss of *grlG* was adaptive under the experimental conditions. Further
784 support of selection acting on *grlG* is the high population level frequency that several of these
785 new mutations reached in their respective lines. On average, the 10 unique SNPs in *grlG* are
786 supported by 61% of the total reads in their respective populations compared to an average of
787 only 41% support for the 28 remaining SNPs in other genes. These data suggest that *grlG*
788 variants increased in abundance due to selection, rather than drift. In addition, by screening
789 multiple additional clones from the experimental lines, we found that variants in the 5' region
790 of *grlG* are significantly associated with the loss of cooperation (non-fruiting) while those in the
791 3' region are not. However, very few of the clones screened in the 3' region carried a variant in
792 *grlG* (9%) and this may have limited our power to detect an association. We were unable to find
793 any non-fruiting clones for evolved lines 11 and 17 but the large proportion of normally fruiting

794 clones that carry a *grlG* variant certainly suggests a lack of an association in those lines. To help
795 us make sense of these results, we next explore the limited amount of currently available
796 information about *grlG* and view our findings in light of what is known more broadly about the
797 large and highly conserved family of proteins, the G protein-coupled receptors (GPCRs).
798
799 The G protein-coupled receptors (GPCRs) in eukaryotes are the largest class of receptors of
800 extracellular stimuli. They generally activate intracellular responses via heterotrimeric G-
801 proteins. In humans there are over 800 GPCR genes making them the most abundant gene
802 family in the human genome (Lagerström and Schiöth 2008). They are involved in a huge
803 diversity of biological processes including signaling of hormones, metabolites and
804 neurotransmitters to cell migration and development (Rosenbaum *et al.* 2009). The GPCRs are
805 responsible for approximately 66 known single-gene human diseases, and they are the target of
806 about one third of FDA-approved drugs (Hauser *et al.* 2017; Schöneberg and Liebscher 2021).
807 Thus, identifying the ligands and the roles of yet uncharacterized GPCRs (or, orphan GPCRs) is of
808 great interest broadly and the GPCRs in *Dictyostelium* are no exception. *Dictyostelium*
809 *discoideum* is an established model system for studying numerous processes such as chemotaxis
810 and other cell-motility linked processes such as phagocytosis and development (Bozzaro 2019),
811 all of which involve GPCRs.
812
813 The *D. discoideum* genome has a surprisingly large and diverse repertoire of more than 55
814 GPCRs (Eichinger *et al.* 2005; Sucgang *et al.* 2011; Heidel *et al.* 2011). Classically the GPCRs are
815 categorized into six classes based on sequence and function (Kolakowski 1994; Bockaert and Pin

816 1999); *D. discoideum* has representative members of most classes (Prabhu and Eichinger 2006).
817 Similar to those in vertebrates, the GPCRs in *D. discoideum* are involved in a diversity of
818 biological processes, including significant roles in development. Most notably, members of the
819 class E GPCRs include the receptors of cAMP (cARs). The chemoattractant cAMP is pivotal in the
820 initiation and coordination of multicellular development in *D. discoideum* (Saran *et al.* 2002;
821 Loomis 2014). Perhaps it is not surprising then that the cAMP receptors were the first GPCRs to
822 be identified (Klein *et al.* 1988) in *D. discoideum* and remain the most extensively studied.
823
824 Some members of the class C GPCRs (which includes *grlG*) in *D. discoideum* have also been
825 implicated in development. The *D. discoideum* genome has 17 members of the class C GPCRs,
826 known as glutamate receptor-like (grl) proteins (Eichinger *et al.* 2005). For most of the group,
827 the ligands, effectors and even the specific signaling pathways remain unknown. A great deal of
828 progress has been made over the past few decades especially after the completion of the *D.*
829 *discoideum* genome in 2005 (Eichinger *et al.* 2005). At least four of the glutamate receptor-like
830 proteins have been described as having roles in development including *grlA* (Prabhu *et al.*
831 2007a; Anjard *et al.* 2009), *grlB* (Wu and Janetopoulos 2013), *grlE* (Anjard and Loomis 2006; Wu
832 and Janetopoulos 2013) and *grlJ* (Prabhu *et al.* 2007b). Moreover, Prabhu *et al.* (2007b) also
833 found that all 17 are expressed throughout development, some with increased expression early
834 in aggregation (*grlA, D, E, J, M, N, Q*) and others with increased expression from the tight
835 aggregate stage and on (including *grlG, B, C, F, H, K, L, O, P, R*). Much remains to be learned but
836 it is easy to conceive that *grlG,* like other members of this protein family in *D. discoideum*, is
837 also involved in cooperation during multicellular development.

838

839 We are aware of only one previous study that investigated the function of *grlG* but it was in the
840 context of predation rather than development. Upon exposure to the chemoattractant folic
841 acid (used by *D. discoideum* to chemotax toward and phagocytose bacteria) Pan *et al.* (2016)
842 identified increased phosphorylation at key serine residues in both *grlG* and *grlL.* Both *grlG* and
843 *grlL* were thus considered candidate folic acid receptors (they referred to them as folic acid
844 receptors ('far') *far2* and *far1,* respectively). However, only *far1* (*grlL*), and not *grlG,* was
845 required for eliciting the response to folic acid and the authors moved forward with the
846 characterization of only *far1* (*grlL*) (Pan *et al.* 2016, 2018). During the work that followed, they
847 noticed that the loss of *far1* (*grlL*) does not completely abolish the response to folic acid and
848 lipopolysaccharide (LPS) which suggests that other proteins are involved. That observation is in
849 line with some earlier studies which also suggested that there are two folic acid receptors, each
850 with a different binding affinity (de Wit and van Haastert 1985; Segall *et al.* 1988). But *grlG* is
851 not required for the folic acid response and there is only limited evidence to support any
852 involvement (Pan *et al.* 2016; Lamrabet *et al.* 2020). We have no reason to believe that the
853 parallel evolution of *grlG* that we have identified is related to the detection or phagocytosis of
854 bacterial prey. The *D. discoideum* AX4 lines were adapted to the laboratory growth and nutrient
855 conditions well before the start of experimental evolution by Kuzdzal-Fick *et al.* (2011). Instead,
856 the primary novelty of the experimental environment was the extreme low-relatedness that
857 favored cheaters.

858

859 The number of large-effect variants in *grlG* suggests that the loss of *grlG* was adaptive under
860 the experimental conditions of low relatedness. What is less clear from our results is why only
861 the variants in the 5' region of *grlG* are significantly associated with non-fruiting and those in
862 the 3' region are not. To investigate, we viewed the amino acid sequence topology and
863 predicted protein structure to investigate other potential explanations **(Figure 5B)**. *GrlG* shares
864 the same major features found in most class C GPCRs including a long 5' extracellular domain, a
865 seven-transmembrane domain toward the 3' end followed by an intracellular C-terminal tail
866 **(Figure 5B)** (Pin *et al.* 2003; Rosenbaum *et al.* 2009). Ligand binding in class C GPCRs typically
867 occurs via a Venus flytrap domain (similar to the ancestral periplasmic binding proteins of
868 bacteria) situated in the 5' extracellular domain (Cao *et al.* 2009; Chun *et al.* 2012). Upon
869 binding its ligand, conformational changes throughout the seven-transmembrane domain lead
870 to the activation of G proteins (or other effectors) at the intracellular C-terminus to induce
871 signaling inside the cell (Rosenbaum *et al.* 2009). Based on sequence homology and the
872 predicted folding structure, *grlG* appears to function similarly. In the predicted structure
873 generated by AlphaFold (Jumper *et al.* 2021; Varadi *et al.* 2022), the extracellular region can be
874 seen folded (with high confidence) into a Venus flytrap structure with a clearly visible cleft, or
875 ligand binding pocket **(Figure 5A)**.
876
877

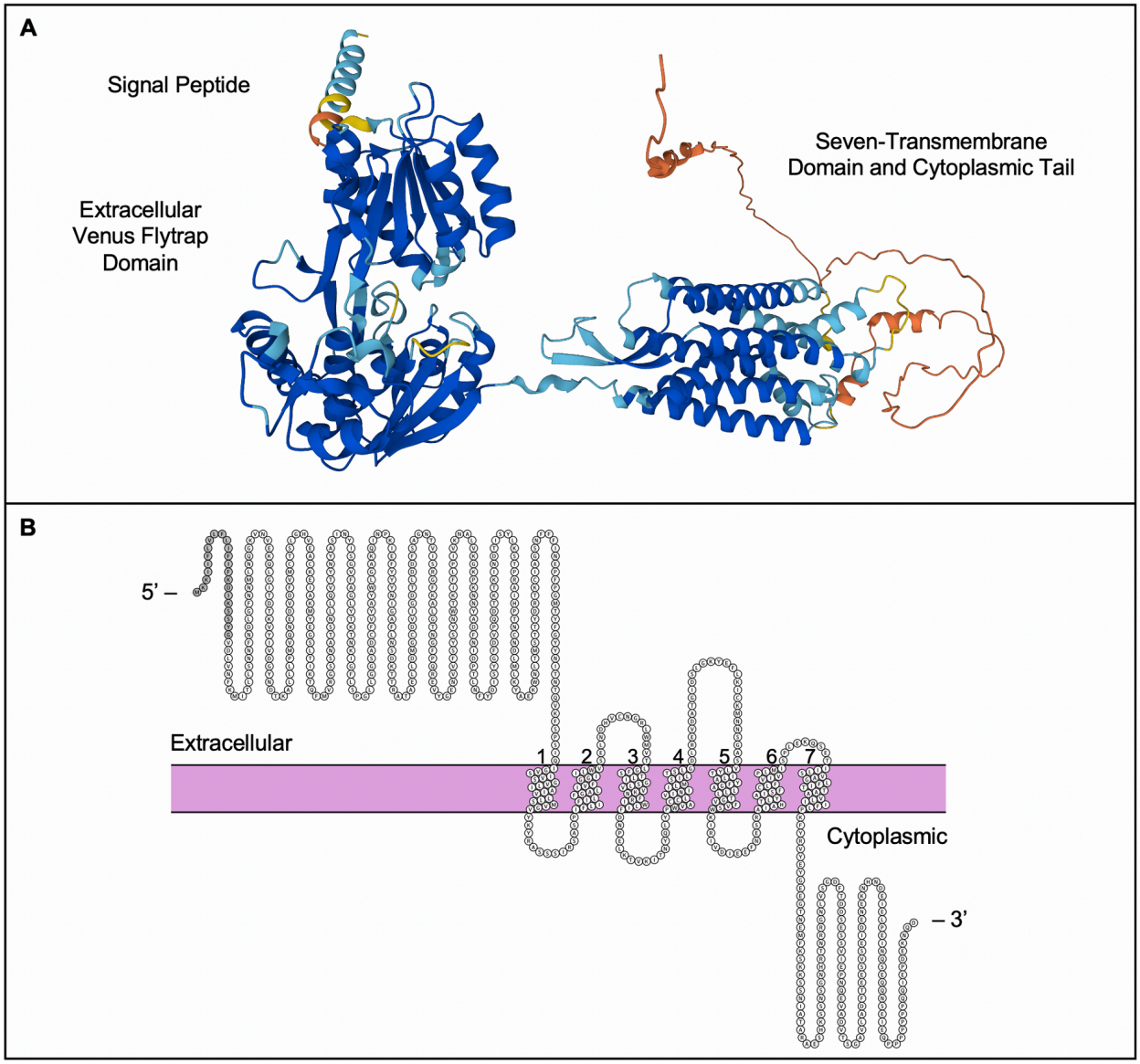


878

879 **Figure 5. Predicted structure and sequence topology of *D. discoideum grlG.* A**. Predicted

880 folding structure of *grlG* generated by AlphaFold (Jumper *et al.* 2021; Varadi *et al.* 2022). Colors

881 indicate the model confidence in the local accuracy; dark blue is very high confidence, light blue

882 is confident, yellow is low confidence and orange is very low confidence. This structure can be

883 be viewed interactively with the 3D viewer on the AlphaFold Protein Structure Database

884 (https://alphafold.ebi.ac.uk/entry/Q75JP4). **B.** The sequence topology of *grlG* generated in

885 Protter (Omasits *et al.* 2014). Extracellular regions are shown above the membrane (in purple)
886 and the cytoplasmic regions below. The 5' amino acids in grey indicate the signal peptide.
887
888
889 According to the amino acid sequence topology**,** each of the four variants that we screened for
890 in the 5' region would result in early protein truncation, either upstream of or within the
891 extracellular binding domain. It is not surprising that the loss of the binding domain, such as in
892 our 5' variants, would render a receptor non-functional. Similar results have been
893 experimentally demonstrated for the homologous protein, *grlL* (*far1*). Pan *et al.* (2018)
894 generated a *grlL* (*far1*) mutant missing only the extracellular binding domain (the remainder of
895 the protein was intact) to demonstrate that the mutant was unable to elicit a response to its
896 ligands. But while we might predict that the large impact variants in the transmembrane
897 domain, particularly those also resulting in early protein truncation, would lead to similar
898 outcomes, our data do not support a significant association between any of the 3' variants and
899 non-fruiting. Additional work is needed to understand how *D. discoideum* cells handle aberrant
900 *grlG* mRNAs and proteins. But even if we assume that aberrant and truncated proteins are not
901 degraded, given the coordinated functionality between extracellular ligand binding and the
902 resultant intracellular signaling, the loss of either end of this transmembrane protein receptor
903 would seem to disable signaling. Moreover, the variants in both regions of *grlG* were positively
904 selected and increased in abundance under the experimental conditions. Although it is difficult
905 to speculate given so many unknowns, perhaps all variants in *grlG* (both 5' and 3') provided the

906 selective advantage of cheating, but only those that inhibit ligand binding are also likely to
907 result in non-fruiting when in isolation.
908
909 Another challenge to interpreting our results is that variants in *grlG* are apparently not
910 completely penetrant. While our results are broadly consistent with variants in 5' *grlG* causing
911 non-fruiting, we did identify a one clone in line 21 that was still able to form a fruiting body
912 despite carrying a variant in 5' *grlG* that introduces a premature stop codon just before the
913 extracellular binding domain. Although human or technical error is a possibility, there also
914 many potential biological explanations. Some of the factors that can influence penetrance
915 include gene expression levels, modifier genes, the co-occurrence of one or more additional
916 variants, the environment or other non-genetic factors (Cooper *et al.* 2013). However, the lack
917 of penetrance we observed may not be explained until we know more about the gene,
918 particularly the ligand(s) it binds and the pathway(s) it is involved in. This brings our attention
919 to the complex and pleiotropic nature of GPCR signaling and highlights the challenge of
920 predicting variant impacts.
921
922 From the great deal of work with GPCRs in humans and disease in particular, it is clear that
923 mutations in membrane proteins can result in a huge variety of impacts. The effect of any
924 mutation will depend on the properties of the protein as well as the type and location of the
925 mutation (Schöneberg and Liebscher 2021; Zaucha *et al.* 2021). Some of the many potential
926 impacts of GPCR mutations include improper membrane trafficking or localization; alterations
927 to critical secondary or tertiary structures; inhibition or altered efficiency of binding ligand(s) or

928 interacting proteins and inhibition or altered efficiency of signaling through downstream
929 effectors. Further complicating matters, some GPCRs bind multiple ligands and/or have
930 multiple effectors. Likewise, one ligand can have multiple receptors. In *D. discoideum* for
931 example, the chemoattractant cAMP has four receptors (cARs 1–4) in the GPCR class E, each of
932 which has a different cAMP-binding affinity and expression pattern. The binding affinity of each
933 cAMP receptor is correlated with the stage of development during which it is expressed to
934 optimally meet the needs of the cell at that time (Kim *et al.* 1996).
935
936 Members of the class C glutamate receptor-like protein family (which includes *grlG*) in *D.*
937 *discoideum* also exemplify complexities of GPCR signaling. *GrlE*, which is the GABA receptor
938 during late development, is also bound by the competitive inhibitor of GABA, glutamate.
939 Depending on which ligand is bound, GABA or glutamate, *grlE* is coupled to a different G
940 protein subunit (Gα7 or Gα9, respectively) (Anjard and Loomis 2006). Sporulation is delayed
941 while glutamate is bound and then induced when displaced and bound by GABA, together
942 ensuring the appropriate timing of sporulation (Anjard and Loomis 2006; Anjard *et al.* 2009).
943 Another example of a glutamate receptor-like protein binding multiple ligands is the folic acid
944 receptor *far1* (otherwise known as *grlL*), which also recognizes lipopolysaccharide (LPS) to
945 mediate chemotaxis and phagocytosis of bacterial prey (Pan *et al.* 2016, 2018). And similar to
946 the previously described multiple receptors of cAMP, other ligands bind multiple glutamate
947 receptor-like proteins of class C as well. While *grlE* is the GABA receptor during late
948 development, *grlB* is instead the GABA receptor during early stages of development (Wu and
949 Janetopoulos 2013). There are also several examples in *D. discoideum* of potential redundancy

950 (or rather, the suspected involvement of multiple receptors) of glutamate receptor-like
951 proteins, wherein the loss of the focal receptor does not completely abolish the response as
952 would be expected if a single receptor were responsible for ligand recognition and response.
953 Examples in which the loss of the focal receptor does not completely abolish the response
954 include the autocrine proliferation repressor protein A (*aprA*) receptor, *grlH* (Tang *et al.* 2018);
955 the phenylthiourea receptor, *grlJ* (Robery *et al.* 2013); and the folic acid (and LPS) receptor, *far1*
956 (*grlL*) (Pan *et al.* 2016, 2018).
957
958 Regarding the potential redundancy of *far1* (*grlL*), as previously mentioned, the involvement of
959 *grlG* has been suggested (Pan *et al.* 2016; Lamrabet *et al.* 2020) but that has little relevance in
960 this study as we have no reason to believe that our results are predation related. However, we
961 do not rule out the possibility *grlG* may also interact with folic acid or another molecule with
962 overlapping roles in bacterial predation as well as in cooperation and fruiting body formation.
963 Given our understanding of the complex nature of GPCR signaling, even if *grlG* was found to be
964 involved in the response to bacterial prey, that would not contradict the evidence we present
965 here suggesting its role in cooperation. Instead, perhaps the knowledge that *grlG* and other
966 members of the glutamate receptor-like protein family sometimes show low levels of
967 overlapping functionality may help explain why the loss of *grlG* in our evolved clones did not
968 always lead to the total loss of cooperation and non-fruiting.
969
970
971 **Conclusion**

972 In this study we returned to cell lines previously evolved under low-relatedness by Kuzdzal-Fick
973 *et al.* (2011) to investigate the genomic changes underlying the observed evolution of non-
974 fruiting obligate cheaters. That study demonstrated how low relatedness in a natural
975 population would lead to a collapse of multicellularity and with it, the advantages of fruiting
976 body formation and spore dispersal. In this study we used whole-genome sequencing and
977 variant analysis of those experimentally evolved *D. discoideum* low-relatedness cell lines. We
978 identified parallel evolution of the orphan GPCR *grlG* as well as another 28 variants in other
979 genes. The genes that we identified with variants are spread throughout the genome and do
980 not share any significantly enriched functions or other annotations. In addition, none of these
981 genes have been previously implicated in cheating or cooperation. The lack of overlap among
982 these genes alone, nor with previously implicated cheater genes, is further testament to the
983 complexity of the social cycle and aggregative multicellularity in *D. discoideum* and further
984 highlights that these processes are orchestrated by a large diversity of genes and pathways.
985
986 The orphan GPCR *grlG* acquired variants of moderate to high impact in more than half of the
987 experimental lines suggesting that the loss of *grlG* was adaptive under the experimental
988 conditions of low-relatedness. By screening additional clones from the evolved lines, we
989 identified a significant correlation between the complete loss of cooperation (inability to form
990 the social stage, a fruiting body) and the presence of variants in the 5' region of *grlG* containing
991 the signal peptide and extracellular binding domain. Our results suggest that *grlG* is one of now
992 two genes (second to *fbxA* (Ennis *et al.* 2000)) to have been implicated in obligate non-fruiting
993 cheating in *D. discoideum*. Although future work is needed to identify the interacting molecules

994 and the precise role of *grlG*, this work adds *grlG* to the growing list of GPCRs in the *D.*
995 *discoideum* genome to have a role in multicellular development. This is noteworthy because it
996 brings us one step closer to deorphanization of the ever-important GPCRs and highlights the
997 need to expand research efforts to characterize the remaining GPCRs in *D. discoideum.*
998
999
1000 ***Acknowledgments***
1001 We thank members of the Queller-Strassmann laboratory for helpful advice on this research
1002 and Jennie Kuzdzal-Fick for making her evolved lines available. This material is based upon work
1003 supported by the National Science Foundation under grant numbers IOS 16-56756 and DEB 17-
1004 53743. Additional funding came from a pilot grant from the McDonnell Genome Institute.
1005
1006
1007 ***Supplemental Materials***
1008 **Supplemental Methods**
1009 **Supplemental Tables**
1010 **Additional File 1.** Results of the limited screening of clones for variants in genes other than *grlG*
1011 **Supplemental Material 1.** Example images of non-fruiting clone morphology
1012 **Supplemental Material 2.** Variant calls that survived filtration from each of the three variant
1013 callers (GATK, Freebayes and Delly), in VCF format
1014 **Supplemental Material 3.** *D. discoideum* gene annotations downloaded from NCBI on 10-25-19

1015 **Supplemental Material 4.** The resulting number of variants after each step of filtration of the
1016 VCF files independently generated by each caller.
1017 **Supplemental Material 5.** Results of the functional annotation clustering with a high
1018 classification efficiency performed for the 29 genes with SNPs using the online tool DAVID
1019 (https://david.ncifcrf.gov/)
1020
1021
1022 **References**


1023 Anjard, C., and W. F. Loomis, 2006 GABA induces terminal differentiation of *Dictyostelium*
1024 through a $GABA_B$ receptor. Development 133: 2253–2261.
1025 Anjard, C., Y. Su, and W. F. Loomis, 2009 Steroids initiate a signaling cascade that triggers rapid
1026 sporulation in *Dictyostelium*. Development 136: 803–812.
1027 Barrick, J. E., and R. E. Lenski, 2013 Genome dynamics during experimental evolution. Nat. Rev.
1028 Genet. 14: 827–839.
1029 Bateman, A., M. J. Martin, S. Orchard, M. Magrane, R. Agivetova *et al.*, 2021 UniProt: The
1030 universal protein knowledgebase in 2021. Nucleic Acids Res. 49: D480–D489.
1031 Benabentos, R., S. Hirose, R. Sucgang, T. Curk, M. Katoh *et al.*, 2009 Polymorphic members of
1032 the lag gene family mediate kin discrimination in *Dictyostelium*. Curr. Biol. 19: 567–572.
1033 Benjamini, Y., and Y. Hochberg, 1995 Controlling the false discovery rate: A practical and
1034 powerful approach to multiple testing. J. R. Stat. Soc. Ser. B Methodol. 57: 289–300.
1035 Bockaert, J., and J. P. Pin, 1999 Molecular tinkering of G protein-coupled receptors: An
1036 evolutionary success. EMBO J. 18: 1723–1729.

1037 Bonner, J. T., 1998 The origins of multicellularity. Integr. Biol. Issues News Rev. 1: 27–36.

1038 Bozzaro, S., 2019 The past, present and future of *Dictyostelium* as a model system. Int. J. Dev.
1039 Biol. 63: 321–331.

1040 Buttery, N. J., C. N. Jack, B. Adu-Oppong, K. T. Snyder, C. R. L. Thompson *et al.*, 2012 Structured
1041 growth and genetic drift raise relatedness in the social amoeba *Dictyostelium*
1042 *discoideum*. Biol. Lett. 8: 794–797.

1043 Buttery, N. J., D. E. Rozen, J. B. Wolf, and C. R. L. Thompson, 2009 Quantification of social
1044 behavior in *D. discoideum* reveals complex fixed and facultative strategies. Curr. Biol. 19:
1045 1373–1377.

1046 Buttery, N. J., J. Smith, D. C. Queller, and J. E. Strassmann, 2013 Measuring cheating, fitness,
1047 and segregation in *Dictyostelium discoideum*, pp. 231–248 in *Dictyostelium discoideum*
1048 *Protocols*, Humana Press, Totowa, NJ.

1049 Cameron, D. L., L. Di Stefano, and A. T. Papenfuss, 2019 Comprehensive evaluation and
1050 characterisation of short read general-purpose structural variant calling software. Nat.
1051 Commun. 10: 1–11.

1052 Cao, J., S. Huang, J. Qian, J. Huang, L. Jin *et al.*, 2009 Evolution of the class C GPCR Venus flytrap
1053 modules involved positive selected functional divergence. BMC Evol. Biol. 9: 1–12.

1054 Cavender, J. C., and K. B. Raper, 1965 The Acrasieae in nature. I. Isolation. Am. J. Bot. 52: 294–
1055 296.

1056 Charette, S. J., and P. Cosson, 2004 Preparation of genomic DNA from *Dictyostelium discoideum*
1057 for PCR analysis. BioTechniques 36: 574–575.

1058 Chun, L., W. H. Zhang, and J. F. Liu, 2012 Structure and ligand recognition of class C GPCRs. Acta
1059 Pharmacol. Sin. 33: 312–323.
1060 Cooper, D. N., M. Krawczak, C. Polychronakos, C. Tyler-Smith, and H. Kehrer-Sawatzki, 2013
1061 Where genotype is not predictive of phenotype: Towards an understanding of the
1062 molecular basis of reduced penetrance in human inherited disease. Hum. Genet. 132:
1063 1077–1130.
1064 Cooper, G. A., and S. A. West, 2018 Division of labour and the evolution of extreme
1065 specialization. Nat. Ecol. Evol. 2: 1161–1167.
1066 Eichinger, L., J. A. Pachebat, G. Glöckner, M. A. Rajandream, R. Sucgang *et al.*, 2005 The genome
1067 of the social amoeba *Dictyostelium discoideum*. Nature 435: 43–57.
1068 Ellegren, H., 2004 Microsatellites: Simple sequences with complex evolution. Nat. Rev. Genet. 5:
1069 435–445.
1070 Ennis, H. L., D. N. Dao, S. U. Pukatzki, and R. H. Kessin, 2000 *Dictyostelium* amoebae lacking an
1071 F-box protein form spores rather than stalk in chimeras with wild type. Proc. Natl. Acad.
1072 Sci. 97: 3292–3297.
1073 Ennis, H. L., D. N. Dao, M. Y. Wu, and R. H. Kessin, 2003 Mutation of the *Dictyostelium fbxA*
1074 gene affects cell-fate decisions and spatial patterning. Protist 154: 419–429.
1075 Fey, P., P. Gaudet, T. Curk, B. Zupan, E. M. Just *et al.*, 2009 dictyBase—a *Dictyostelium*
1076 bioinformatics resource update. Nucleic Acids Res. 37: D515–D519.
1077 Flowers, J. M., S. I. Li, A. Stathos, G. Saxer, E. A. Ostrowski *et al.*, 2010 Variation, sex, and social
1078 cooperation: Molecular population genetics of the social amoeba *Dictyostelium*
1079 *discoideum*. PLoS Genet. 6: 1–14.

1080 Fortunato, A., D. C. Queller, and J. E. Strassmann, 2003a A linear dominance hierarchy among
1081 clones in chimeras of the social amoeba *Dictyostelium discoideum*. J. Evol. Biol. 16: 438–
1082 445.
1083 Fortunato, A., J. E. Strassmann, L. Santorelli, and D. C. Queller, 2003b Co-occurrence in nature
1084 of different clones of the social amoeba, *Dictyostelium discoideum*. Mol. Ecol. 12: 1031–
1085 1038.
1086 Foster, K. R., G. Shaulsky, J. E. Strassmann, D. C. Queller, and C. R. L. Thompson, 2004 Pleiotropy
1087 as a mechanism to stabilize cooperation. Nature 431: 693–696.
1088 Garrison, E., Z. N. Kronenberg, E. T. Dawson, B. S. Pedersen, and P. Prins, 2021 Vcflib and tools
1089 for processing the VCF variant call format. bioRxiv 2021.05.21.445151.
1090 Garrison, E., and G. Marth, 2012 Haplotype-based variant detection from short-read
1091 sequencing.
1092 Gilbert, O. M., K. R. Foster, N. J. Mehdiabadi, J. E. Strassmann, and D. C. Queller, 2007 High
1093 relatedness maintains multicellular cooperation in a social amoeba by controlling
1094 cheater mutants. Proc. Natl. Acad. Sci. U. S. A. 104: 8913–8917.
1095 Gilbert, O. M., J. E. Strassmann, and D. C. Queller, 2012 High relatedness in a social amoeba:
1096 The role of kin-discriminatory segregation. Proc. R. Soc. B Biol. Sci. 279: 2619–2624.
1097 Grosberg, R. K., and R. R. Strathmann, 2007 The evolution of multicellularity: A minor major
1098 transition? Annu. Rev. Ecol. Evol. Syst. 38: 621–654.
1099 Gruenheit, N., K. Parkinson, B. Stewart, J. A. Howie, J. B. Wolf *et al.*, 2017 A polychromatic
1100 “greenbeard” locus determines patterns of cooperation in a social amoeba. Nat.
1101 Commun. 8: 1–9.

1102 Hamilton, W. D., 1964 The genetical evolution of social behaviour. II. J. Theor. Biol. 7: 17–52.

1103 Hardin, G., 1968 The tragedy of the commons. Science 162: 1243–1248.

1104 Hauser, A. S., M. M. Attwood, M. Rask-Andersen, H. B. Schiöth, and D. E. Gloriam, 2017 Trends
1105 in GPCR drug discovery: New agents, targets and indications. Nat. Rev. Drug Discov. 16:
1106 829–842.

1107 Heidel, A. J., H. M. Lawal, M. Felder, C. Schilde, N. R. Helps *et al.*, 2011 Phylogeny-wide analysis
1108 of social amoeba genomes highlights ancient origins for complex intercellular
1109 communication. Genome Res. 21: 1882–1891.

1110 Hirose, S., R. Benabentos, H. I. Ho, A. Kuspa, and G. Shaulsky, 2011 Self-recognition in social
1111 amoebae is mediated by allelic pairs of tiger genes. Science 333: 467–470.

1112 Hirose, S., B. Santhanam, M. Katoh-Kurosawa, G. Shaulsky, and A. Kuspa, 2015 Allorecognition,
1113 via *tgrB1* and *tgrC1*, mediates the transition from unicellularity to multicellularity in the
1114 social amoeba *Dictyostelium discoideum*. Development 142: 3561–3570.

1115 Ho, H. I., S. Hirose, A. Kuspa, and G. Shaulsky, 2013 Kin recognition protects cooperators against
1116 cheaters. Curr. Biol. 23: 1590–1595.

1117 Huang, D. W., B. T. Sherman, and R. A. Lempicki, 2009a Bioinformatics enrichment tools: Paths
1118 toward the comprehensive functional analysis of large gene lists. Nucleic Acids Res. 37:
1119 1–13.

1120 Huang, D. W., B. T. Sherman, and R. A. Lempicki, 2009b Systematic and integrative analysis of
1121 large gene lists using DAVID bioinformatics resources. Nat. Protoc. 4: 44–57.

1122 Jumper, J., R. Evans, A. Pritzel, T. Green, M. Figurnov *et al.*, 2021 Highly accurate protein
1123 structure prediction with AlphaFold. Nature 596: 583–589.

1124 Kessin, R. H., 2001 *Dictyostelium: evolution, cell biology, and the development of*
1125 *multicellularity*. Cambridge University Press.
1126 Khare, A., and G. Shaulsky, 2010 Cheating by exploitation of developmental prestalk patterning
1127 in *Dictyostelium discoideum*. PLoS Genet. 6: e1000854.
1128 Kim, J., P. V. Haastert, and P. N. Devreotes, 1996 Social senses: G-protein-coupled pathways in
1129 *Dictyostelium*. Chem. Biol. 3: 239–243.
1130 Klein, P. S., T. J. Sun, C. L. Saxe, A. R. Kimmel, L. Ronald *et al.*, 1988 A chemoattractant receptor
1131 controls development in *Dictyostelium discoideum*. Science 241: 1467–1472.
1132 Knoll, A. H., 2011 The multiple origins of complex multicellularity. Annu. Rev. Earth Planet. Sci.
1133 39: 217–239.
1134 Kolakowski, L. F., 1994 GCRDb: A G-protein-coupled receptor database. Receptors Channels 2:
1135 1–7.
1136 Kosugi, S., Y. Momozawa, X. Liu, C. Terao, M. Kubo *et al.*, 2019 Comprehensive evaluation of
1137 structural variation detection algorithms for whole genome sequencing. Genome Biol.
1138 20: 8–11.
1139 Kuspa, A., and W. F. Loomis, 1992 Tagging developmental genes in *Dictyostelium* by restriction
1140 enzyme-mediated integration of plasmid DNA. Proc. Natl. Acad. Sci. U. S. A. 89: 8803–
1141 8807.
1142 Kuzdzal-Fick, J. J., S. A. Fox, J. E. Strassmann, and D. C. Queller, 2011 High relatedness is
1143 necessary and sufficient to maintain multicellularity in *Dictyostelium*. Science 334:
1144 1548–1551.

1145 Lagerström, M. C., and H. B. Schiöth, 2008 Structural diversity of G protein-coupled receptors
1146 and significance for drug discovery. Nat. Rev. Drug Discov. 7: 339–357.
1147 Lamrabet, O., A. Melotti, F. Burdet, N. Hanna, J. Perrin *et al.*, 2020 Transcriptional responses of
1148 *Dictyostelium discoideum* exposed to different classes of bacteria. Front. Microbiol. 11:
1149 1–12.
1150 Li, H., 2011 A statistical framework for SNP calling, mutation discovery, association mapping
1151 and population genetical parameter estimation from sequencing data. Bioinformatics
1152 27: 2987–2993.
1153 Li, H., 2013 Aligning sequence reads, clone sequences and assembly contigs with BWA-MEM.
1154 Li, H., and R. Durbin, 2009 Fast and accurate short read alignment with Burrows-Wheeler
1155 transform. Bioinformatics 25: 1754–1760.
1156 Li, H., B. Handsaker, A. Wysoker, T. Fennell, J. Ruan *et al.*, 2009 The Sequence Alignment/Map
1157 format and SAMtools. Bioinformatics 25: 2078–2079.
1158 Loomis, W. F., 2014 Cell signaling during development of *Dictyostelium*. Dev. Biol. 391: 1–16.
1159 Loomis, W. F., 2015 Genetic control of morphogenesis in *Dictyostelium*. Dev. Biol. 402: 146–
1160 161.
1161 Madgwick, P. G., B. Stewart, L. J. Belcher, C. R. L. Thompson, and J. B. Wolf, 2018 Strategic
1162 investment explains patterns of cooperation and cheating in a microbe. Proc. Natl. Acad.
1163 Sci. U. S. A. 115: E4823–E4832.
1164 Mahmoud, M., N. Gobet, D. I. Cruz-Dávalos, N. Mounier, C. Dessimoz *et al.*, 2019 Structural
1165 variant calling: The long and the short of it. Genome Biol. 20: 1–14.

1166 McKenna, A., M. Hanna, E. Banks, A. Sivachenko, K. Cibulskis *et al.*, 2010 The genome analysis
1167 toolkit: A MapReduce framework for analyzing next-generation DNA sequencing data.
1168 Genome Res. 20: 1297–1303.
1169 McLaren, W., L. Gil, S. E. Hunt, H. S. Riat, G. R. S. Ritchie *et al.*, 2016 The Ensembl Variant Effect
1170 Predictor. Genome Biol. 17: 122.
1171 Mehdiabadi, N. J., C. N. Jack, T. T. Farnham, T. G. Platt, S. E. Kalla *et al.*, 2006 Kin preference in a
1172 social microbe. Nature 442: 881–882.
1173 Mehdiabadi, N. J., M. R. Kronforst, D. C. Queller, and J. E. Strassmann, 2009 Phylogeny,
1174 reproductive isolation and kin recognition in the social amoeba *Dictyostelium*
1175 *purpureum*. Evol. Int. J. Org. Evol. 63: 542–8.
1176 Noh, S., L. Christopher, J. E. Strassmann, and D. C. Queller, 2020 Wild *Dictyostelium discoideum*
1177 social amoebae show plastic responses to the presence of nonrelatives during
1178 multicellular development. Ecol. Evol. 10: 1119–1134.
1179 Noh, S., K. S. Geist, X. Tian, J. E. Strassmann, and D. C. Queller, 2018 Genetic signatures of
1180 microbial altruism and cheating in social amoebas in the wild. Proc. Natl. Acad. Sci. U. S.
1181 A. 115: 3096–3101.
1182 de Oliveira, J. L., A. C. Morales, B. Stewart, N. Gruenheit, J. Engelmoer *et al.*, 2019 Conditional
1183 expression explains molecular evolution of social genes in a microbe. Nat. Commun. 10:
1184 1–12.
1185 Omasits, U., C. H. Ahrens, S. Müller, and B. Wollscheid, 2014 Protter: Interactive protein feature
1186 visualization and integration with experimental proteomic data. Bioinformatics 30: 884–
1187 886.

1188 Ostrowski, E. A., 2019 Enforcing cooperation in the social amoebae. Curr. Biol. 29: R474–R484.

1189 Pan, M., M. P. Neilson, A. M. Grunfeld, P. Cruz, X. Wen *et al.*, 2018 A G-protein-coupled
1190 chemoattractant receptor recognizes lipopolysaccharide for bacterial phagocytosis. PLoS
1191 Biol. 16: 1–20.

1192 Pan, M., X. Xu, Y. Chen, and T. Jin, 2016 Identification of a chemoattractant G-protein-coupled
1193 receptor for folic acid that controls both chemotaxis and phagocytosis. Dev. Cell 36:
1194 428–439.

1195 Pin, J. P., T. Galvez, and L. Prézeau, 2003 Evolution, structure, and activation mechanism of
1196 family 3/C G-protein-coupled receptors. Pharmacol. Ther. 98: 325–354.

1197 Prabhu, Y., and L. Eichinger, 2006 The *Dictyostelium* repertoire of seven transmembrane
1198 domain receptors. Eur. J. Cell Biol. 85: 937–946.

1199 Prabhu, Y., S. Mondal, L. Eichinger, and A. A. Noegel, 2007a A GPCR involved in post aggregation
1200 events in *Dictyostelium discoideum*. Dev. Biol. 312: 29–43.

1201 Prabhu, Y., R. Müller, C. Anjard, and A. A. Noegel, 2007b *GrlJ*, a *Dictyostelium* $GABA_B$-like
1202 receptor with roles in post-aggregation development. BMC Dev. Biol. 7: 1–14.

1203 Queller, D. C., 2000 Relatedness and the fraternal major transitions. Philos. Trans. R. Soc. B Biol.
1204 Sci. 355: 1647–1655.

1205 Queller, D. C., E. Ponte, S. Bozzaro, and J. E. Strassmann, 2003 Single-gene greenbeard effects in
1206 the social amoeba *Dictyostelium discoideum*. Science 299: 105–106.

1207 Queller, D. C., and J. E. Strassmann, 2018 Evolutionary conflict. Annu. Rev. Ecol. Evol. Syst. 49:
1208 73–93.

1209 Rausch, T., T. Zichner, A. Schlattl, A. M. Stütz, V. Benes *et al.*, 2012 DELLY: Structural variant
1210 discovery by integrated paired-end and split-read analysis. Bioinformatics 28: i333–i339.
1211 Robery, S., R. Tyson, C. Dinh, A. Kuspa, A. A. Noegel *et al.*, 2013 A novel human receptor
1212 involved in bitter tastant detection identified using *Dictyostelium discoideum*. J. Cell Sci.
1213 126: 5465–5476.
1214 Robinson, J. T., H. Thorvaldsdóttir, A. M. Wenger, A. Zehir, and J. P. Mesirov, 2017 Variant
1215 review with the integrative genomics viewer. Cancer Res. 77: e31–e34.
1216 Robinson, J. T., H. Thorvaldsdóttir, W. Winckler, M. Guttman, E. S. Lander *et al.*, 2011
1217 Integrative genomics viewer. Nat. Biotechnol. 29: 24–26.
1218 Rosenbaum, D. M., S. G. F. Rasmussen, and B. K. Kobilka, 2009 The structure and function of G-
1219 protein-coupled receptors. Nature 459: 356–363.
1220 Santorelli, L. A., A. Kuspa, G. Shaulsky, D. C. Queller, and J. E. Strassmann, 2013 A new social
1221 gene in *Dictyostelium discoideum*, *chtB*. BMC Evol. Biol. 13: 1–10.
1222 Santorelli, L. A., C. R. L. Thompson, E. Villegas, J. Svetz, C. Dinh *et al.*, 2008 Facultative cheater
1223 mutants reveal the genetic complexity of cooperation in social amoebae. Nature 451:
1224 1107–1110.
1225 Saran, S., M. E. Meima, E. Alvarez-Curto, K. E. Weening, D. E. Rozen *et al.*, 2002 cAMP signaling
1226 in *Dictyostelium*: Complexity of cAMP synthesis, degradation and detection. J. Muscle
1227 Res. Cell Motil. 23: 793–802.
1228 Sathe, S., N. Khetan, and V. Nanjundiah, 2014 Interspecies and intraspecies interactions in social
1229 amoebae. J. Evol. Biol. 27: 349–362.

1230 Schöneberg, T., and I. Liebscher, 2021 Mutations in G protein–coupled receptors: Mechanisms,
1231 pathophysiology and potential therapeutic approaches. Pharmacol. Rev. 73: 89–119.
1232 Scott, T. J., and D. C. Queller, 2019 Long-term evolutionary conflict, Sisyphean arms races, and
1233 power in Fisher's geometric model. Ecol. Evol. 9: 11243–11253.
1234 Sebé-Pedrós, A., B. M. Degnan, and I. Ruiz-Trillo, 2017 The origin of Metazoa: A unicellular
1235 perspective. Nat. Rev. Genet. 18: 498–512.
1236 Segall, J. E., A. A. Bominaar, E. Wallraff, and R. J. De Wit, 1988 Analysis of a *Dictyostelium*
1237 chemotaxis mutant with altered chemoattractant binding. J. Cell Sci. 91 ( Pt 4): 479–489.
1238 smith, J., D. C. Queller, and J. E. Strassmann, 2014 Fruiting bodies of the social amoeba
1239 *Dictyostelium discoideum* increase spore transport by *Drosophila*. BMC Evol. Biol. 14: 1–
1240 5.
1241 smith, J., J. E. Strassmann, and D. C. Queller, 2016 Fine-scale spatial ecology drives kin selection
1242 relatedness among cooperating amoebae. Evolution 70: 848–859.
1243 Srivastava, S., A. K. Avvaru, D. T. Sowpati, and R. K. Mishra, 2019 Patterns of microsatellite
1244 distribution across eukaryotic genomes. BMC Genomics 20: 1–14.
1245 Strassmann, J. E., O. M. Gilbert, and D. C. Queller, 2011 Kin discrimination and cooperation in
1246 microbes. Annu. Rev. Microbiol. 65: 349–67.
1247 Strassmann, J. E., and D. C. Queller, 2011 Evolution of cooperation and control of cheating in a
1248 social microbe. Proc. Natl. Acad. Sci. U. S. A. 108 Suppl: 10855–62.
1249 Strassmann, J. E., Y. Zhu, and D. C. Queller, 2000 Altruism and social cheating in the social
1250 amoeba *Dictyostelium discoideum*. Nature 408: 965–967.

1251 Sucgang, R., A. Kuo, X. Tian, W. Salerno, A. Parikh *et al.*, 2011 Comparative genomics of the
1252 social amoebae *Dictyostelium discoideum* and *Dictyostelium purpureum*. Genome Biol.
1253 12: R20.
1254 Tan, A., G. R. Abecasis, and H. M. Kang, 2015 Unified representation of genetic variants.
1255 Bioinformatics 31: 2202–2204.
1256 Tang, Y., Y. Wu, S. E. Herlihy, F. J. Brito-Aleman, J. H. Ting *et al.*, 2018 An autocrine proliferation
1257 repressor regulates *Dictyostelium discoideum* proliferation and chemorepulsion using
1258 the G protein-coupled receptor *grlH*. mBio 9: e02443-17.
1259 Tarasov, A., A. J. Vilella, E. Cuppen, I. J. Nijman, and P. Prins, 2015 Sambamba: Fast processing
1260 of NGS alignment formats. Bioinformatics 31: 2032–2034.
1261 Tenaillon, O., A. Rodríguez-Verdugo, R. L. Gaut, P. McDonald, A. F. Bennett *et al.*, 2012 The
1262 molecular diversity of adaptive convergence. Science 335: 457–461.
1263 Thompson, C. R. L., Q. Fu, C. Buhay, R. R. Kay, and S. Gad, 2004 A bZIP/bRLZ transcription factor
1264 required for DIF signaling in *Dictyostelium*. Development 131: 513–523.
1265 Tian, X., J. E. Strassmann, and D. C. Queller, 2011 Genome nucleotide composition shapes
1266 variation in simple sequence repeats. Mol. Biol. Evol. 28: 899–909.
1267 Tóth, G., Z. Gáspári, and J. Jurka, 2000 Microsatellites in different eukaryotic genomes: Surveys
1268 and analysis. Genome Res. 10: 967–981.
1269 Tsutsui, N. D., 2004 Scents of self: The expression component of self/non-self recognition
1270 systems. Ann. Zool. Fenn. 41: 713–727.

1271 Van den Bergh, B., T. Swings, M. Fauvart, and J. Michiels, 2018 Experimental design, population
1272 dynamics, and diversity in microbial experimental evolution. Microbiol. Mol. Biol. Rev.
1273 82: e00008-18.
1274 Varadi, M., S. Anyango, M. Deshpande, S. Nair, C. Natassia *et al.*, 2022 AlphaFold Protein
1275 Structure Database: Massively expanding the structural coverage of protein-sequence
1276 space with high-accuracy models. Nucleic Acids Res. 50: D439–D444.
1277 West, S. A., A. S. Griffin, A. Gardner, and S. P. Diggle, 2006 Social evolution theory for
1278 microorganisms. Nat. Rev. Microbiol. 4: 597–607.
1279 de Wit, R. J. W., and P. J. M. van Haastert, 1985 Binding of folates to *Dictyostelium discoideum*
1280 cells. Demonstration of five classes of binding sites and their interconversion. Biochim.
1281 Biophys. Acta Biomembr. 814: 199–213.
1282 Wolf, J. B., J. A. Howie, K. Parkinson, N. Gruenheit, D. Melo *et al.*, 2015 Fitness trade-offs result
1283 in the illusion of social success. Curr. Biol. 25: 1086–1090.
1284 Wu, Y., and C. Janetopoulos, 2013 Systematic analysis of γ-aminobutyric acid (GABA)
1285 metabolism and function in the social amoeba *Dictyostelium discoideum*. J. Biol. Chem.
1286 288: 15280–15290.
1287 Zaucha, J., M. Heinzinger, A. Kulandaisamy, E. Kataka, Ó. L. Salvádor *et al.*, 2021 Mutations in
1288 transmembrane proteins: Diseases, evolutionary insights, prediction and comparison
1289 with globular proteins. Brief. Bioinform. 22:.
1290

1291 **Table 1. Number of SNPs and average read depth by sample.** Whole-genome sequencing and
1292 variant analysis resulted in 38 SNPs called in 25 of the 47 samples and distributed throughout

1293 17 of the 24 evolved lines. This table indicates the number of SNPs called for each sample. The
1294 average mapped read depth was calculated for the raw reads normalized by the length of all
1295 annotated genes. Samples from each evolved line, sequenced as populations, are simply
1296 numbered 1 - 24. Clonal samples isolated from each of the evolved lines are named according
1297 to the population number hyphenated with the non-fruiting clone ID (*e.g.,* "NF1"). The non-
1298 fruiting clone IDs were retained for record keeping purposes; they are not related to the
1299 number of clones sequenced for a line.

| Sample | SNP Count | Average Mapped Read Depth |
|---|---|---|
| 1 | 0 | 128 |
| 1-NF2 | 0 | 43 |
| 2 | 1 | 137 |
| 3 | 0 | 146 |
| 3-NF1 | 1 | 127 |
| 4 | 0 | 171 |
| 5 | 0 | 161 |
| 5-NF2 | 3 | 40 |
| 6 | 1 | 152 |
| 7 | 4 | 229 |
| 7-NF2 | 5 | 44 |
| 8 | 0 | 165 |
| 8-NF1 | 0 | 89 |
| 9 | 1 | 220 |
| 9-NF3 | 1 | 24 |
| 10 | 1 | 151 |
| 10-NF3 | 1 | 23 |

| | | |
|---|---|---|
| 11 | 2 | 116 |
| 11-NF1 | 0 | 37 |
| 12 | 1 | 215 |
| 12-NF1 | 1 | 97 |
| 13 | 1 | 165 |
| 13-NF2 | 1 | 70 |
| 14 | 0 | 127 |
| 14-NF3 | 0 | 22 |
| 15 | 0 | 176 |
| 15-NF1 | 0 | 69 |
| 16 | 0 | 277 |
| 16-NF2 | 3 | 118 |
| 17 | 3 | 123 |
| 18 | 0 | 191 |
| 18-NF1 | 3 | 30 |
| 19 | 0 | 319 |
| 19-NF1 | 0 | 80 |
| 20 | 0 | 231 |
| 20-NF1 | 1 | 66 |
| 20-NF3 | 1 | 32 |
| 21 | 1 | 272 |
| 21-NF1 | 3 | 40 |
| 21-NF2 | 5 | 45 |
| 22 | 3 | 291 |
| 23 | 0 | 305 |
| 23-NF1 | 0 | 25 |

| | | |
|---|---|---|
| 23-NF2 | 0 | 43 |
| 24 | 0 | 222 |
| 24-NF1 | 1 | 32 |
| 1 | 0 | 128 |

1300

1301

1302 **Table 2. List of called SNPs and the impacted locus.** Whole-genome sequencing and variant
1303 analysis resulted in this list of 38 bi-allelic SNPs impacting 29 different genes. For each SNP this
1304 table provides the precise location in the genome and the Dictybase gene ID (followed by gene
1305 name when available), followed by the called samples. Samples from each evolved line,
1306 sequenced as populations, are simply numbered 1–24. Clonal samples isolated from each of the
1307 evolved lines are named according to the population number hyphenated with the non-fruiting
1308 clone ID (*e.g.,* "NF1"). The last two columns of the table are the variant consequence and the
1309 estimated impact rating made by the Ensembl Variant Effect Predictor (VEP) (VEP 95.3).

| **Chrom:Site** | **Gene ID** | **Called Sample(s)** | **VEP Consequence** | **VEP Impact** |
|---|---|---|---|---|
| NC_007087.3:2556092 | DDB_G0269332 | 22 | missense_var. | Moderate |
| NC_007087.3:3010110 | DDB_G0270828 | 21-NF1 | missense_var. | Moderate |
| NC_007087.3:3624901 | DDB_G0270964 | 18-NF1 | missense_var. | Moderate |
| NC_007087.3:3928085 | DDB_G0269956(RTE) | 21-NF2 | upstream_gene_var. | Modifier |
| NC_007087.3:4563335 | DDB_G0270834(*sgmA*) | 5-NF2 | missense_var. | Moderate |
| NC_007088.5:1741979 | DDB_G0272244(*grlG*) | 6 | stop_gained | High |
| NC_007088.5:1741982 | DDB_G0272244(*grlG*) | 7 & 7-NF2 | missense_var. | Moderate |
| NC_007088.5:1742043 | DDB_G0272244(*grlG*) | 11 | missense_var. | Moderate |

| | | | | |
|---|---|---|---|---|
| NC_007088.5:1742355 | DDB_G0272244(*grlG*) | 17 | missense_var. | Moderate |
| NC_007088.5:1742362 | DDB_G0272244(*grlG*) | 13 & 13-NF2 | missense_var. | Moderate |
| NC_007088.5:1742375 | DDB_G0272244(*grlG*) | 10 & 10-NF3 | stop_gained | High |
| NC_007088.5:1742506 | DDB_G0272244(*grlG*) | 18-NF1 | missense_var. | Moderate |
| NC_007088.5:1743478 | DDB_G0272244(*grlG*) | 2 | missense_var. | Moderate |
| NC_007088.5:1743823 | DDB_G0272244(*grlG*) | 21 & 21-NF2 | stop_gained | High |
| NC_007088.5:1743844 | DDB_G0272244(*grlG*) | 22 | stop_gained | High |
| NC_007088.5:1761939 | DDB_G0272484 | 16-NF2 | missense_var. | Moderate |
| NC_007088.5:4313995 | DDB_G0274875(*rnf160*) | 16-NF2 | stop_gained | High |
| NC_007088.5:6565220 | DDB_G0276291 | 17 | missense_var. | Moderate |
| NC_007088.5:6762467 | DDB_G0276367 | 17 | stop_gained | High |
| NC_007088.5:6787007 | DDB_G0276529 | 7-NF2 & 16-NF2 | missense_var. | Moderate |
| NC_007088.5:6871012 | DDB_G0276553 | 7 & 7-NF2 | upstream_gene_var. | Modifier |
| NC_007088.5:7954466 | DDB_G0277481 | 21-NF2 | missense_var. | Moderate |
| NC_007089.4:1029309 | DDB_G0278531 | 24-NF1 | stop_gained | High |
| NC_007089.4:1073554 | DDB_G0278559 | 7 & 7-NF2 | missense_var. | Moderate |
| NC_007089.4:1101637 | DDB_G0278575 | 7 & 7-NF2 | upstream_gene_var. | Modifier |
| NC_007089.4:3459101 | DDB_G0280505(*tmem144A*) | 5-NF2 | missense_var. | Moderate |
| NC_007089.4:5126190 | DDB_G0281923(*mrhA*) | 21-NF1 | downstream_gene_var. | Modifier |
| NC_007089.4:5671190 | DDB_G0282355 | 12 & 12-NF1 | upstream_gene_var. | Modifier |
| NC_007090.3:2549009 | DDB_G0284845(*gxcC*) | 3-NF1 | upstream_gene_var. | Modifier |
| NC_007091.3:1993104 | DDB_G0288805 | 22 | stop_gained | High |
| NC_007091.3:2942727 | DDB_G0289555(*arkA*) | 21-NF1 | missense_var. | Moderate |
| NC_007091.3:2996049 | DDB_G0289583 | 11 | missense_var. | Moderate |
| NC_007091.3:4205385 | DDB_G0290523 | 21-NF2 | synonymous_var. | Low |

| | | | | |
|---|---|---|---|---|
| NC_007091.3:4793752 | DDB_G0290943(*pks39*) | 20-NF1 & 20-NF3 | missense_var. | Moderate |
| NC_007091.3:4956884 | DDB_G0291085(*gxcE*) | 21-NF2 | missense_var. | Moderate |
| NC_007091.3:905736 | DDB_G0287967 | 18-NF1 | downstream_gene_var. | Modifier |
| NC_007092.3:1299121 | DDB_G0292198(RTE) | 5-NF2 | missense_var. | Moderate |
| NC_007092.3:1984519 | DDB_G0292696(*colA*) | 9 & 9-NF3 | missense_var. | Moderate |